Geotechnical and Geological Engineering (2005) 23: 721–756
DOI 10.1007/s10706-004-2899-z

Modelling subsurface heterogeneity by coupled Markov chains: Directional dependency, Walther's law and entropy

A.M.M. ELFEKI[1,*] and F.M. DEKKING[2]
[1]*Water Resources Section, Faculty of Civil Engineering and Geosciences, Delft University of Technology, P.O. Box 5048, 2600 GA Delft, The Netherlands. e-mail: a.m.elfeki@citg.tudelft.nl*
[2]*Faculty of Electrical Engineering, Mathematics and Computer Science, Department of Probability and Statistics, Delft University of Technology, P.O. Box 5031, 2600GA Delft, The Netherlands. e-mail: f.m.dekking@math.tudelft.nl*

Abstract. This paper is an extension of the two-dimensional coupled Markov chain model developed by Elfeki and Dekking (2001) supplemented with extensive simulations. We focus on the development of various coupled Markov chains models: the so-called fully forward Markov chain, fully backward Markov chain and forward–backward Markov chain models. We addressed many issues such as: sensitivity analysis of optimal sampling intervals in horizontal and lateral directions, directional dependency, use of Walther's law to describe lateral variability, effect of conditioning on number of boreholes on the model performance, stability of the Monte Carlo realizations, various implementation strategies, use of cross validation techniques to evaluate model performance and image division for statistically non-homogeneous deposits are addressed. The applications are made on three sites; two sites are located in the Netherlands, and the third is in the USA. The purpose of these applications is to show under which conditions the Markov models can be used, and to provide some guidelines for the practice. Entropy maps are good tools to indicate places where high uncertainty is present, so can be used for designing sampling networks to reduce uncertainty at these locations. Symmetric and diagonally dominant horizontal transition probabilities with proper sampling interval show plausible results (fits with geologists prediction) in terms of delineation of subsurface heterogeneous structures. Walther's law can be utilised with a proper sampling interval to account for the lateral variability.

Key words. Markov chains, Walthers' law, conditional simulations, entropy, stochastic modelling, subsurface heterogeneity.

1. Introduction

The impact of heterogeneities in the subsurface is critical to understand the movement of contaminants and the possibility for their removal by various remediation technologies. Therefore, characterization of subsurface heterogeneity that incorporates the dominant features of the geological heterogeneity at the significant scales of

*Corresponding author: Water Resources Section, Faculty of Civil Engineering and Geosciences, Delft University of Technology, P.O. Box 5048, 2600 GA Delft, The Netherlands. e-mail: a.m.elfeki@citg.tudelft.nl

variability is essential for reliable predictions of the contaminant fate. Several geostatistical methods are available such as stochastic Gaussian fields based on autocorrelations or variograms (e.g., Deutsh and Journel, 1992), object based models (e.g., Haldorsen and Damsleth, 1990; Chessa, 1995), fractal models (e.g., Haldorsen and Damsleth, 1990; Wheatcraft and Cushman, 1990) and transition probability based geo-statistical models (e.g., Markov chains). The early work on Markov chains was performed by Krumbein (1967) to simulate stratigraphic sequences in one-dimension. For recent work on extensions of Markov chains to multi-dimensions see Carle and Fogg, 1996; Carle, et al., 1998; Parks, et al., 2000; Elfeki and Dekking, 2001.

The coupled Markov chain model (CMC) developed by Elfeki and Dekking (2001) has some advantages over conventional semivariogram-based methods. These advantages include: (1) Conventional geostatistical methods (Deutsch and Journel 1992) have difficulty incorporating geologic interpretations. This is possible with the CMC method. (2) The CMC method does not need parametric fitting of variograms, auto-covariance or transition probabilities like conventional geostatistical methods (Deutsch and Journel, 1992). It works directly, with transition probability data estimated from boreholes. (3) The CMC method can straightforwardly deal with statistical non-homogeneities. Variability—either statistically homogeneous or heterogeneous—can be implemented in a single transition probability matrix, and the algorithm will cope with this variability in the data. However, in other methods, some preprocessing such as zonation and parameter estimation of each zone is needed (see e.g., the sequential indicator simulation applied by Bierkens, 1994 to the central Rhine-Meuse delta in The Netherlands). (4) Asymmetric heterogeneity structures can be modeled by CMC because there is no intrinsic symmetry assumption in the coupled Markov chain model. In contrast, variogram or autocovariance based geostatistics handle only symmetric heterogeneity. (5) Geological observations and principles (e.g., fining up/down sequences and juxtapositional tendencies) can be directly implemented in the transition probability matrix. (6) CMC methodology needs only the single step transition probability matrix in both horizontal and vertical directions, which can be obtained from the field with high degree of reliability, and the algorithm takes care of the N-step transition probabilities (larger lags). However, in variogram or autocovariance based geostatistics estimation of variogram or auto-covariance at all possible lags is needed, and the reliability deteriorates at larger lags.

The coupled Markov chain model developed seems promising when applied to outcrop data (Elfeki and Dekking, 2001). However, some issues need to be resolved. For instance, transition probabilities of the chains are directionally dependent, i.e., the transition probability from one state to another in a specific direction, e.g., from left to right, is not necessarily the same as going from right to left. So the model needs further investigation when applied to field data. The issue of directionality, the estimation of the horizontal transition probabilities, sampling intervals in the horizontal direction, and evaluation of the model performance are crucial aspects for

simulation of realistic field situations. Some of these aspects can be obtained from geological principles (e.g., geological history, sedimentation directions, aggression transgression periods, Walther's law, etc.). This prior knowledge leads to a stochastic-geologic type of approach to subsurface characterization that produces more realistic simulations.

In this paper we present three different types of Markov chain models that can be applied in field situations. These models are based on previous work by Elfeki and Dekking (2001). We also show how one could choose between these models to match specific geological settings. The first model is called the fully forward model, where the name refers to the fact that the transitions are directed from left to right during the estimation phase from field data, and also during the simulation phase. This forward model starts from the most left side well and conditions on right hand side wells. The second model is the fully backward Markov chain model, where the model starts from the right hand side well and goes backward (i.e., to the left) in the direction opposite to the former model. The conditioning is performed on the left side wells. The third model is the forward–backward model, which combines the two approaches. We fill the domain between two wells from both sides in two steps: a forward step which goes from left to right using a forward Markov chain and a second step which goes from right to left using the backward chain. The switching between the two models continues until the domain between the two wells is filled with the geological states.

The layout of the paper is as follows: A brief review of the one-dimensional Markov chain is given followed by the backward Markov chain theory, and an introduction to the coupled Markov chain in two-dimensions. The implementation algorithm of the various Markov chain strategies is presented. The largest part of the paper is devoted to four case studies with two data sets from The Netherlands and one data set from the USA.

2. Theory of One-dimensional Markov Chain

For the sake of completeness a short description of the one-dimensional Markov chain (Doveton, 1994) is given. A Markov chain is a probabilistic model that exhibits a special type of dependence (Billingsley, 1995): given the present the future does not dependent on the past. In formulas, let $Z_0, Z_1, Z_2, \ldots, Z_N$ be a sequence of random variables taking values in the state space $\{S_1, S_2, \ldots, S_n\}$. The sequence is a Markov chain or Markov process, if

$$\begin{aligned} &\Pr(Z_i = S_k | Z_{i-1} = S_l, Z_{i-2} = S_n, Z_{i-3} = S_r, \ldots, Z_0 = S_a) \\ &\quad = \Pr(Z_i = S_k | Z_{i-1} = S_l) =: P_{lk}, \end{aligned} \tag{1}$$

where the symbol '|' is the symbol for conditional probability and p_{ek} is the probability to make a transition from state S_l to S_k.

In one-dimensional problems a Markov chain is described by a transition probability matrix. Transition probabilities correspond to relative frequencies of transitions from states to states. The transition probabilities are all non-negative, and for

fixed l adding the probabilities p_{lk} over all possible states k gives 1. Apart from these single step transitions (i.e., going from one state in a cell to another state in the immediate next cell), one also considers N-step transitions, which stand for transitions from a state to another taking place in N steps. The N-step transition probabilities can be obtained by multiplying the single-step transition probability matrix by itself N times. Krumbein (1967) was the first to simulate stratigraphic sequences in one-dimension using this theory.

The backward (reverse) chain is obtained by reversing the direction in which we go through the cells. Hence its transition probabilities are given by

$$\overleftarrow{p}_{kl} = \Pr(Z_{i-1} = S_l | Z_i = S_k). \tag{2}$$

Actually we do not need an expression for these transition probabilities since we are always interested in conditioning. It will appear in Section 3 that we can express the necessary probabilities in those of the forward chain (see also the appendix).

It is important to notice that the distinction between forward and backward transition probabilities is not trivial (i.e., $p_{lk} \neq \overleftarrow{p}_{kl}$). This property is appealing form geological point of view since sometimes some transitions do exit in certain direction while do not appear in other directions (juxtapositional tendencies). This phenomenon will be illustrated in the application section.

3. One-dimensional Markov Chain Conditioned on Future States

Consider a one-dimensional series of events that is Markovian (Figure 1). Fixing a cell i with its state Z_i, we will refer to a state Z_j for any $j > i$ as future state. The probability of cell 1 to be in state S_b, given that the previous cell 0 is in state S_a and cell N is in state S_q can be expressed mathematically as (Elfeki and Dekking, 2001)

$$p_{ab|q} := \Pr(Z_1 = S_b | Z_0 = S_a,\ Z_N = S_q) = \frac{p_{ab} p_{bq}^{(N-1)}}{p_{aq}^{(N)}}, \tag{3}$$

where $p_{aq}^{(N)}$ is the N-step transition probability.

We will now compute the corresponding conditional probability for the backward chain:

$$\overleftarrow{p}_{qr|a} = \Pr(Z_{N-1} = S_r | Z_N = S_q,\ Z_0 = S_a).$$

This probability can be written in terms of joint probabilities as

$$\overleftarrow{p}_{qr|a} = \Pr(Z_{N-1} = S_r | Z_N = S_q, Z_0 = S_a) = \frac{\Pr(Z_{N-1} = S_r, Z_N = S_q, Z_0 = S_a)}{\Pr(Z_N = S_q, Z_0 = S_a)}. \tag{4}$$

Switching to conditional probabilities leads to

S_a	S_b			S_l	S_k	S_d		S_r	S_q
0	1	2		i-1	i	i+1		N-1	N

Figure 1. Numbering series of events for a one-dimensional Markov chain, row 1 shows the states, and row 2 shows the spatial locations.

$$\overleftarrow{p}_{qr|a} = \Pr(Z_{N-1} = S_r | Z_N = S_q,\ Z_0 = S_a)$$
$$= \frac{\Pr(Z_N = S_q | Z_{N-1} = S_r, Z_0 = S_a).\Pr(Z_{N-1} = S_r | Z_0 = S_a).\Pr(Z_0 = S_a)}{\Pr(Z_N = S_q | Z_0 = S_a).\Pr(Z_0 = S_a)}. \quad (5)$$

By applying the Markovian property on the conditional probability in the numerator of Equation (5), one obtains

$$\overleftarrow{p}_{qr|a} = \Pr(Z_{N-1} = S_r | Z_N = S_q, Z_0 = S_a)$$
$$= \frac{\Pr(Z_N = S_q | Z_{N-1} = S_r).\Pr(Z_{N-1} = S_r | Z_0 = S_a)}{\Pr(Z_N = S_q | Z_0 = S_a)} = \frac{P_{rq} P_{ar}^{(N-1)}}{P_{aq}^{(N)}}, \quad (6)$$

and we have expressed $\overleftarrow{p}_{qr|a}$ in the forward transition probabilities.

4. Coupling and Conditioning Two One-dimensional Markov Chains on a Lattice System (CMC Method)

The CMC is based on two independent Markov chains. One describes the variations in the lithologies in the horizontal direction, and the other describes the variation in the vertical direction (from top to bottom). Although the method is general, it can handle any direction. The reason for choosing the top to bottom transitions is that it is easy to find information on the top surface layers where this information can be propagated down via the CMC model. The two chains are coupled in the sense that a state Z_{ij} of a cell (i, j) in the domain depends on states $Z_{i,\,j-1}$ and $Z_{i-1,\,j}$ of the cells on top $(i, j-1)$ and on the left $(i-1, j)$ of the current cell. We follow the same procedure as in our previous work for coupling the vertical and the horizontal chains. This means that when we use the forward model, the forward horizontal chain is coupled with the vertical chain using the formula, Elfeki and Dekking (2001)

$$P_{lm,\,k|q} := \Pr(Z_{i,\,j} = S_k | Z_{i-1,\,j} = S_l, Z_{i,\,j-1} = S_m, Z_{N_x,\,j} = S_q)$$
$$= \frac{p_{lk}^{h}.p_{kq}^{h(N_x - i)}.p_{mk}^{v}}{\sum_f p_{lf}^{h}.p_{fq}^{h(N_x - i)}.p_{mf}^{v}}, \quad k = 1, \ldots, n, \quad (7)$$

where p_{lk}^{h} is the one-step forward horizontal transition probability from S_l to S_k (the superscript h refers to the horizontal direction), $p_{kq}^{h(N_x - i)}$ is the $(N_x - i)$-step forward horizontal transition probability from S_k to S_q, and p_{mk}^{v} is the one-step vertical transition probability from S_m to S_k (the superscript v refers to the vertical direction).

However, when we apply the backward chain in the horizontal direction, the backward transition probability matrix is used to replace the forward one. Therefore, the formula becomes

$$\overleftarrow{p}_{dm,\,k|a} := \Pr(Z_{i,\,j} = S_k | Z_{i-1,\,j} = S_d, Z_{i,\,j-1} = S_m, Z_{0,\,j} = S_a)$$
$$= \frac{p_{kd}^{h}.p_{ak}^{h(i)}.p_{mk}^{v}}{\sum_f p_{fd}^{h}.p_{af}^{h(i)}.p_{mf}^{v}}, \quad k = 1, \ldots, n. \quad (8)$$

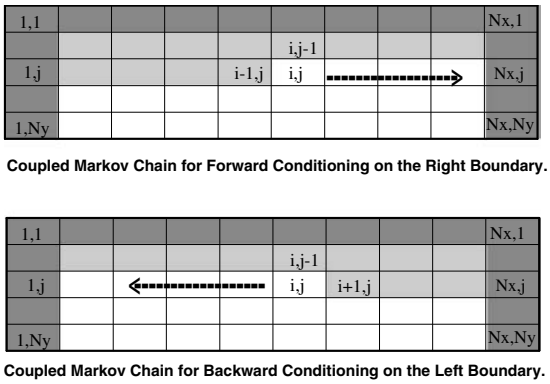

Figure 2. Numbering system in a two-dimensional domain with forward and backward conditioning: dark grey cells are known cells, light grey cells are previously generated cells, and white cells are cells that are going to be generated.

Finally, in case of the forward-backward Markov chain model the above formulas are used in an alternating manner. In the forward steps Equation (7) is used, while in the backward steps Equation (8) is used (Figure 2).

5. Extracting a Single Final Geological Image from a Collection of Generated Realizations

An "engineering approach" is adopted to extract an image of the final lithology from a collection of realizations generated by the CMC model in a Monte Carlo framework. This final image is obtained by choosing the lithology that occurs most frequently in the set of realizations. The background that motivated this approach is two fold: the first is that the subsurface structure is a single realization, therefore we tried to extract the most probable image of the subsurface from a collection of realizations. The second is that engineers prefer cost effective techniques, So, instead of generating many realizations of subsurface structures and perform flow and transport simulations in each realization, we propose an alternative approach: one summarizes all generated realizations, and obtains a single most probable image that can be used later as a deterministic image for flow and transport predictions saving a lot of computational costs. This approach has been used by Elfeki and Rajabiani (2002) and shows promising results.

This approach is as follows. The indicator function of lithology S_k at cell (i, j) is given by

$$I_k(i,j) = \begin{cases} 1 & \text{if } Z_{ij} = S_k, \\ 0 & \text{otherwise.} \end{cases} \tag{9}$$

Let the realizations be numbered 1, ... , MC, and let $Z_{i,j}^{(R)}$ be the lithology of cell (i, j) in the R^{th} realization. The empirical relative frequency of lithology S_k at cell (i,j) is:

$$\pi_{ij}^{k} = \frac{1}{MC} \sum_{R=1}^{MC} I_k^{(R)}(i,\ j). \tag{10}$$

In the final image Z^* the lithology at cell (i, j) will be the lithology which occurs most frequently in the MC realizations. So, if S_l is such that

$$\pi_{ij}^{l} = \max\left\{\pi_{ij}^{1}, \pi_{ij}^{2}, \ldots, \pi_{ij}^{n}\right\} \tag{11}$$

then $Z_{i,\,j}^{*} = S_l$. In Equation (11) it may happen that l is not unique; in that case the computer code chooses the first lithology S_l with maximal occurrence. This phenomenon—if it happens at all—will only take place at the boundaries between lithologies and will have negligible influence on the results.

An application of the aforementioned method is presented in the following example, which is one of the case studies (Afsluitdijk-Lemmer) given later. Figure 4 presents three generated realizations conditioned on eight boreholes. Figure 5 shows the relative frequency plots of each lithology.

6. Empirical Entropy

Adopting the approach mentioned in Section 5 to decide for a final image that describes the most probable subsurface structure, we found it is necessary to provide some measure of the uncertainty in the final image. We have chosen for empirical entropy to convey this issue. The empirical entropy (see e.g., Arndt, 2001, p. 54) at location (i, j) is given by

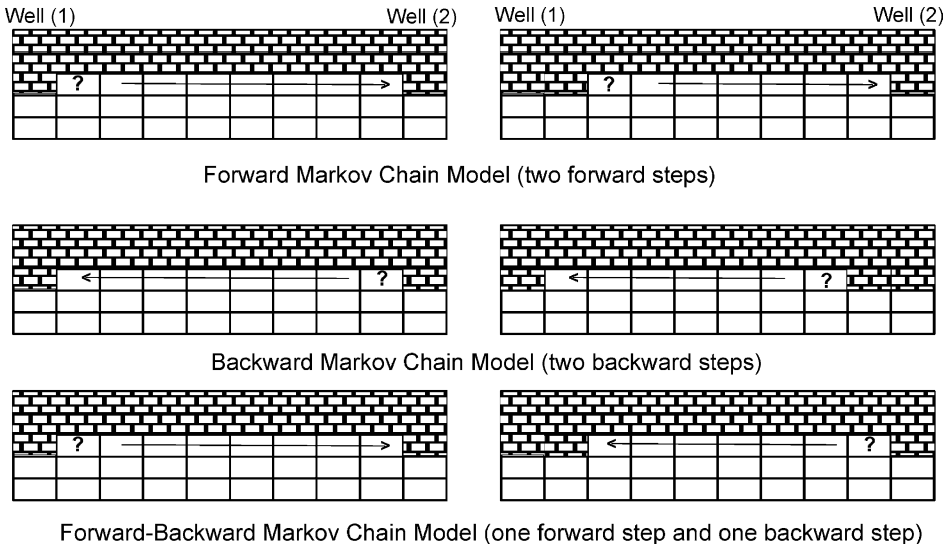

Figure 3. Various ways of implementing Markov chain models: top is the fully forward model, middle the fully backward model and down the forward-backward model.

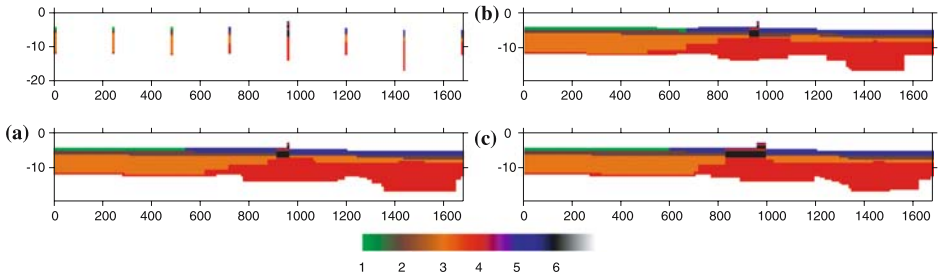

Figure 4. Three realizations generated by the Forward Markov chain model and conditioned on eight boreholes.

$$H_{ij} = -\sum_{k=1}^{n} \pi_{ij}^{k} \ln(\pi_{ij}^{k}), \quad i = 1, \ldots, N_x, \quad j = 1, \ldots, N_y. \tag{12}$$

This formula is implemented in the computer code to calculate the empirical entropy at each grid cell. Therefore a complete map of the entropy distribution can be constructed.

7. Estimation of the Vertical Transition Probability Matrix from Boreholes

The vertical transition probability matrix can be estimated from boreholes data. The tally matrix of vertical transitions is obtained by superimposing a vertical line with equidistant points along the boreholes with a chosen sampling interval. The empirical transition frequencies between the states are calculated by counting how many times a given state say S_l is followed a state S_k, and then divided by the total number of transitions form state S_l to any of the possible states (Davis, 1986)

$$p_{lk}^{v} = T_{lk}^{v} \left(\sum_{q=1}^{n} T_{lq}^{v} \right)^{-1}, \tag{13}$$

where T_{lk}^{v} is the number of observed transitions from S_l to S_k in the vertical direction.

A computer code developed in the present study is utilized to calculate the vertical transition probabilities from boreholes. All boreholes are combined under the assumption that the formation is statistically homogeneous. However, in the applications, we show cases where the method can handle straightforwardly geological features that are statistically non-homogeneous, without using zone subdivisions as other methods (see the sequential indicator simulation method (SIS), applied by Bierkens (1994) on river deposits in the Netherlands).

8. Horizontal Transition Probability Matrix (Walther's Law in a Markovian Context)

One of the important issues in geology and geostatistics is the inference of lateral (horizontal plan) variability. This is made possible by the application of Walther's

law, which states that lithologies that are observed in the vertical depositional sequences must also be deposited in adjacent transects at another scale (Middleton, 1973 referenced by Parks et al. (2000)). This law can be interpreted as: the observed variability in the boreholes at a certain scale (e.g., in the order of cm–m) in the boreholes must be present in the horizontal direction at a larger scale (e.g., in the order of 10 m to km). The scale ratio, which we call Walther's constant, is a key issue in subsurface characterization. In the case studies given in this paper we investigated this issue at three different sites.

9. The Algorithm

A procedure for Monte–Carlo sampling to implement the three Markov chain models is presented. Refer to Figure 3 during the description of the algorithm. The procedure for conditional simulation on two neighbouring wells is as follows. Let the number of simulations MC be given, as well as the horizontal and transition probability matrices (see Sections 7 and 8) and borehole data.

–Fully forward coupled Markov chain model

Step 1: The two-dimensional domain is discretized using proper sampling intervals. The proper sampling interval should be the one that reproduces the important geological features observed in the boreholes with reasonable computer cost (i.e., not very fine that needs high computer cost and not too coarse that smears out important geological features).

Step 2: If there are m boreholes, borehole data is inserted in their locations at (i_k, j), for $k = 1, \ldots, m$ and $j = 1, \ldots, N_y$.

Step 3: The top row is generated using the one-dimensional conditioned horizontal Markov chain at location $(i,1)$, $i = 1, \ldots, N_x$ using Equation (3), i.e., from

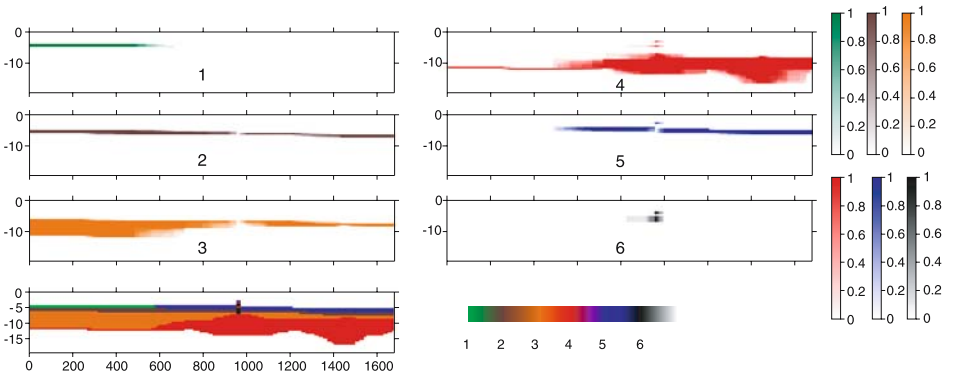

Figure 5. Relative frequency plot of each geological state (three rows) and the final geological image (bottom left corner) based on 30 realizations. The vertical scale bars code the magnitude of the probability of the presence of each of the six geological states.

the conditional distribution Pr $(Z_{i,1} = S_k | Z_{i-1,1} = S_l, Z_{N_x,1} = S_q)$ given state S_l at (i–1, 1) is known and state S_q at cell (N_x, 1). A state is simulated for S_k at cell (i, 1) according to the distribution given by $(p_{l,\, r|q} : r = S_1, \ldots, S_n)$.

Step 4: The rest of the cells (numbered (i, j), $i = 2, \ldots, i_1 - 1, i_1 + 1, \ldots, i_2 - 1, i_2 + 1, \ldots, N_x - 1$ and $j = 2, \ldots, N_y$) is generated inside the domain row-wise, using the conditional distribution Pr $(Z_{i,\,j} = S_k | Z_{i-1,\,j} = S_l, Z_{i,\,j-1} = S_m, Z_{N_x,\,j} = S_q)$, given that the states at (i–1, j), (i, j–1) and (N_x, j) are known. The four-index conditional probability $p_{lm,\,k|q}$ is calculated with Equation (7). From state S_l at the horizontal neighbouring cell (i–1, j), S_m at the vertical neighbouring cell (i, j–1) and the state S_q at the cell on the right hand side boundary (N_x,j) one can determine the succeeding state S_k at cell (i, j). A state S_k is simulated according to the distribution given by $(p_{lm,\, r|q} : r = S_1, \ldots, S_n)$.

Step 5: The procedure stops after having visited all the cells in the domain between the two boreholes at $i = 1$ and $i = N_x$.

Step 6: The same procedure is followed for the next two boreholes and so on, until the domain is filled with the states.

Step 7: After the first realization is generated, the procedure is repeated MC times, starting with different seeds for the random number generator.

Step 8: During the Monte–Carlo runs, the program calculates the empirical probability of presence of a certain lithology at each cell using Equation (11), and the empirical entropy using Equation (12).

–Fully backward coupled Markov chain model

The procedure is similar to the one described above. However, the algorithm starts from right to left, and Equation (8) is used.

–Forward–Backward coupled Markov chain model

The procedure is similar to the one described above. However, the algorithm starts from left to right with one step (the forward-step) using Equation (7). Then, the algorithm starts from right to left in the second step (the backward step) using Equation (8). In this way, the algorithm continuous, switching between forward and backward steps.

10. Sensitivity Analysis, Implementation Issues and Applications

The main reasons to perform research in the application of the coupled Markov chains are: (1) to show the performance of the model in various geological environments; (2) to study the influence of changing model parameters on simulation results to find the best choice of these parameters; (3) to explore the impact of directionality of the CMC (i.e., fully forward, fully backward and forward–backward) on model results. Therefore, the following issues will be considered:

–various sampling intervals,
–various horizontal transition probability matrices,
–various degrees of diagonal dominancy of the horizontal transition matrix,
–use of Walther's law to account for horizontal variability,
–effect of conditioning on the model performance,
–sensitivity of the Monte–Carlo realizations,
–various implementation strategies: forward, backward and forward–backward methods,
–use of cross validation to evaluate the model performance.

In this section, the various coupled Markov chain models described in the previous sections are applied on field data to show under which conditions these models can be used, and to provide some guidelines for the practice. Data from the Netherlands and USA are used. Data from The Netherlands are obtained from CPT (cone penetration tests) profiles from geo-technical projects (Afsluitdijk-Lemmer and Afsluitdiujk Caspar de Roblesdijk). The data from the USA are boreholes at Delaware's river and its underlying aquifer system in the vicinity of the Camden metropolitan area, New Jersey. The data are used for hydro-geological applications and obtained from the literature (Navoy, 1991). The applications show a wide range of variability, starting from simple layering to more complex geological configurations.

10.1. SITE DESCRIPTION AND PARAMETER ESTIMATION

The first application is made at Afsluitdijk-Lemmer which is a part of the IJsselmeerdijken at the province of Friesland, in the north of The Netherlands. A longitudinal section of the dyke from 34 to 38 km is given in Figure 6 (top left most image). The figure shows CPT profiles and the expected geological configuration drawn by geologists. Six different geological lithologies are distinguished. The description of these lithologies and their coding are given in Table 1.

A two-dimensional model for the longitudinal section, shown in Figure 6 (top left most image), is made. The model covers an area of 1680 m $\times$ 20 m and the size of the regular grid used is 168×40 (total of 6720 cells) with cell dimensions of 10 m $\times$ 0.5 m. The vertical transition probability matrix calculated from eight boreholes from top to bottom is given in Table 2. It is important to mention that the white space above the geological cross section of Figure 5 (top) is considered as an artificial lithology coded as state number 7 and the white space under the section is coded as state number 8. So, in total we deal with eight states, two of which are artificial. This is necessary to simulate the top and bottom boundary profile of the geological section.

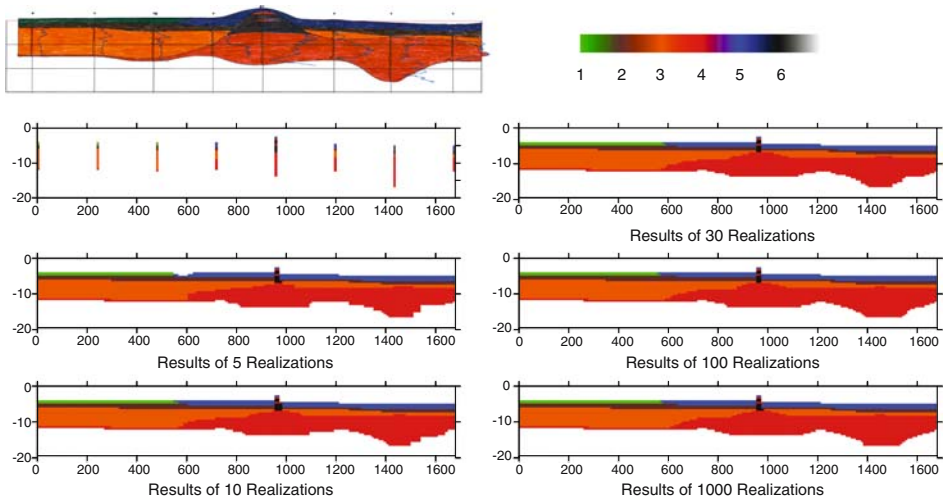

Figure 6. Effect of number of Monte Carlo realizations on the stability of the final image. Geological interpretation (left most top image), second row left most image: borehole data. The rest of the images are generated by the model and conditioned on eight boreholes using 5, 10, 30 100 and 1000 realizations, respectively.

10.2. STABILITY OF MONTE–CARLO REALIZATIONS

A sensitivity analysis was performed to study the effect of number of realizations on the convergence of the final image. To this end, Monte–Carlo simulations with 5, 10, 30, 100 and 1000 realizations were carried out. The results are displayed in Figure 6. It is obvious that the results stabilize at 30 realizations. So, it is decided to choose 30 realizations for the rest of the applications.

10.3. DEGREE OF DIAGONAL DOMINANCY OF THE HORIZONTAL TRANSITION PROBABILITY MATRIX

Several horizontal transition probability matrices are used to find out the best among five matrices in representing the geological structure at the site. Horizontal transition probability matrices are assumed diagonally dominant (i.e., the diagonal elements are larger than the sum of the elements in the row). Diagonal elements of the horizontal transition probability matrix p_{ii}^{h}=0.60, 0.70, 0.80, 0.90 and 0.993 are

Table 1. Coding of lithologies

Lithology	Code
Clay, sandy to sand, clayey (deposition of Duinkerke,Westland – formation)	1
Peat (Hollandpeat, Westland – formation)	2
Sand, locally humous and / with loam layers (formation of Twente)	3
Sand , locally loamy (formation of Drente)	4
Mainly clay (artificial ground)	5
Loam, frequently with sand and stones (formation of Drente)	6

Table 2. Vertical transition probability matrix estimated from eight boreholes sampled over 0.5 m (all boreholes depths are 20 m)

	State							
State	1	2	3	4	5	6	7	8
1	0.500	0.500	0.000	0.000	0.000	0.000	0.000	0.000
2	0.000	0.500	0.500	0.000	0.000	0.000	0.000	0.000
3	0.000	0.000	0.844	0.156	0.000	0.000	0.000	0.000
4	0.000	0.000	0.000	0.830	0.000	0.034	0.000	0.136
5	0.000	0.308	0.000	0.077	0.615	0.000	0.000	0.000
6	0.000	0.000	0.000	0.333	0.000	0.667	0.000	0.000
7	0.045	0.000	0.000	0.000	0.076	0.000	0.879	0.000
8	0.000	0.000	0.000	0.000	0.000	0.000	0.000	1.000

investigated. The off-diagonal elements in each case are calculated based on $p_{ij}^h = (1 - p_{ii}^h)/(n-1)$ where n is the number of states ($n = 7$). This assumption means that the transition from a lithology to itself is dominant, and if there is a change, then there is no information on which change (all equiprobable). This is the worst case scenario when information is lacking about the site in terms of transition probabilities. This approach is similar to the common application of geo-statistics where a single indicator variogram model is used for all components. The horizontal sampling interval is kept constant at 10 m. Figure 7 shows the results of this study. Choosing $p_{ii}^h = 0.993$ on the diagonal elements of the horizontal transition probability matrix, leads to results very close to what has been predicted by the geologists (Figure 6 top left most image), except maybe for the hill in the middle of the image. The problem of the heap is solved by reducing the white space above the profile. This is done by omitting the white space up to the highest borehole. The corresponding vertical transition probabilities are estimated. The only change in the matrix is in the seventh row (see Table 3). Figure 7 bottom row shows the simulation results that correspond to the change made in row number seven. It is obvious that the heap is better reproduced in the simulation.

10.4. SAMPLING INTERVALS (CELL SIZES)

A sensitivity analysis has been performed to look at the horizontal sampling intervals. We want to test a highly diagonal dominancy horizontal matrix with different sampling intervals. The question is which horizontal sampling interval would reproduce the geological features? The vertical sampling interval is kept constant. The vertical and horizontal transition probability matrices are also kept constant (Table 2 for the vertical and table 3 for the horizontal after changing row 7 as in Table 4). Table 3 shows that a lithology followed by itself are dominating, and if there is a change then all the states are equiprobable. Five horizontal sampling intervals are considered. Figure 8 shows the simulations with sampling intervals

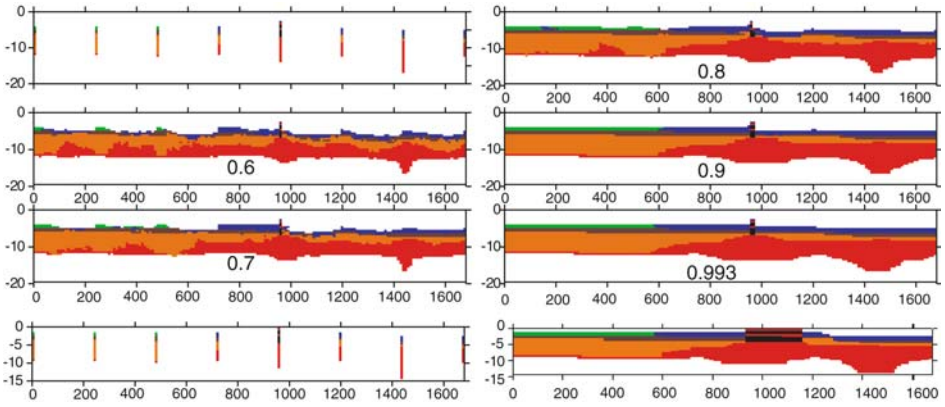

Figure 7. Sensitivity analysis on the degree of diagonal dominancy of the horizontal transition probability matrix. Top left most image is eight boreholes with 20 m depth. The images with p_{ii}^{h}=0.6, 0.7, 0.8, 0.9, 0.993, respectively, are the images generated by the model based on 30 realizations and conditioned on 8 boreholes using horizontal symmetric and diagonally dominant transition probability matrices. Last row left image is eight boreholes with 5 m sky deleted. The right image is the corresponding simulation with 0.993 as diagonal elements.

equal to 2.5, 5, 10, 20 and 40 m, respectively, in the right column and the corresponding entropy maps in the left column. The results lead to more or less the same configuration. However, at small sampling intervals dx = 2.5 and 5 m some white spots appear in the middle of the image (that correspond to state 7) which is an artefact. The reason that this occurs is that in the horizontal transition probability matrix (Table 3) there is a possibility to go from states 6 to 7 with the very low probability 0.001. Therefore there will be a non-negligible chance that 6 might be followed by 7 in a long row of transitions (which do occur in the small sampling interval case). To get rid of this phenomenon, we must put $p_{67}^{h} = 0$. The entropy maps (Figure 8 left column top two images and bottom two images) show reduction in the uncertainty after this correction. This means that incorporating deterministic knowledge ($p_{67}^{h} = 0$) leads to reduction of uncertainty, which is to be expected.

Table 3. Assumed forward horizontal transition probability matrix over a sampling interval of 10 m

	State							
State	1	2	3	4	5	6	7	8
1	0.993	0.001	0.001	0.001	0.001	0.001	0.001	0.001
2	0.001	0.993	0.001	0.001	0.001	0.001	0.001	0.001
3	0.001	0.001	0.993	0.001	0.001	0.001	0.001	0.001
4	0.001	0.001	0.001	0.993	0.001	0.001	0.001	0.001
5	0.001	0.001	0.001	0.001	0.993	0.001	0.001	0.001
6	0.001	0.001	0.001	0.001	0.001	0.993	0.001	0.001
7	0.001	0.001	0.001	0.001	0.001	0.001	0.993	0.001
8	0.001	0.001	0.001	0.001	0.001	0.001	0.001	0.993

Table 4. Estimation of vertical transition probability of state 7 from eight boreholes sampled over 0.5 m for boreholes depth 20 m and 15 m respectively

	State							
State	1	2	3	4	5	6	7	8
7 (20 m depth)	0.045	0.000	0.000	0.000	0.076	0.000	0.879	0.000
7 (15 m depth)	0.012	0.000	0.000	0.000	0.160	0.000	0.720	0.000

10.5. WALTHER'S LAW

We tried to incorporate knowledge from Walther's law in our model. We used the estimated vertical transition probability matrix to describe the horizontal variation between the states. Figure 9 (second row image) is the generated final image based on this matrix. One observes some abrupt changes in the image, caused by the

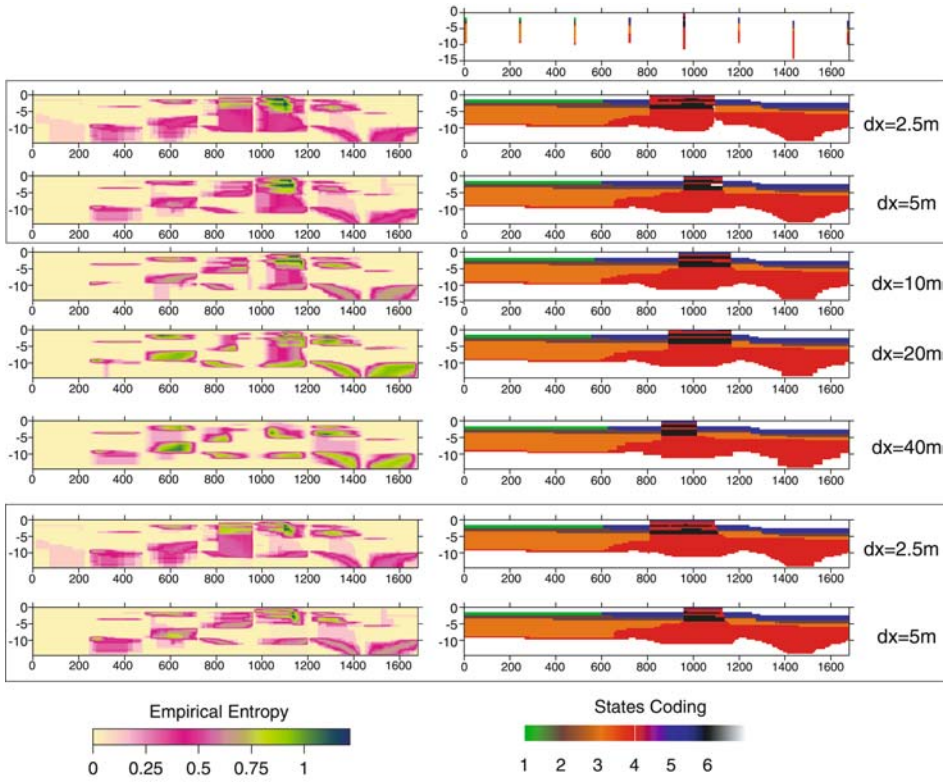

Figure 8. Sensitivity analysis on horizontal sampling intervals using a fixed symmetric horizontal transition probability matrix with diagonal elements p_{ii}^h=0.993. Top right most image shows the eight boreholes, and the rest of the images are the images generated by the model based on 30 realizations, and conditioned on eight boreholes with different horizontal sampling intervals (right column), and empirical entropy estimation (left column). Last two rows are simulations with p_{67}^h=0.

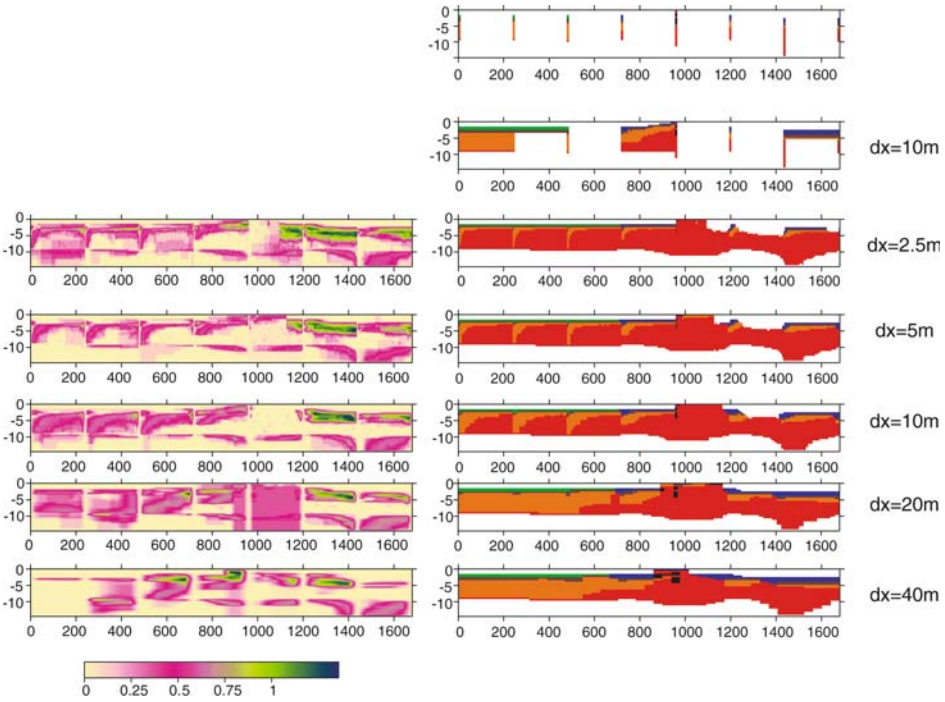

Figure 9. Sensitivity analysis on the application of Walther's Law. The second row shows the generated image using identical horizontal, and vertical transition probability matrices at horizontal sampling intervals of 10 m. The rest shows the generated images with a subtle modification of the vertical transition probability (Table 5) for application in the horizontal direction, with different sampling intervals (ranging from 2.5, 5, 10, 20 and 40 m, respectively,). The right column shows the simulations, and the left column shows the empirical entropy maps.

conditioning. However, when a subtle modification is made in the horizontal transition matrix displayed in Table 5 by changing some zeros to very small probabilities, equal to 0.001, the abrupt changes disappear. The simulations show that with $dx = 40$ m one gets the best results by use of Walther's law.

10.6. SITE DESCRIPTION AND PARAMETER ESTIMATION

The second application is made at Afsluitdijk Caspar de Roblesdijk, which is a part of Waddenzeedijken in the province of Friesland, in the north of the Netherlands. A longitudinal section of the dyke of about 2500 m length is given in Figure 10 (top). Figure 10 shows CPT profiles and the expected geological configuration drawn by geologists. Eleven different geological lithologies are observed in the boreholes. There are also two artificial lithologies added to represent the upper and lower regions of the section. These artificial lithologies are coded with 12 and 13. CPT data as shown in the profiles (Figure 10) are made at different

Table 5. Modified vertical transition probability matrix for use in the horizontal direction (application of Walther's law)

	State							
State	1	2	3	4	5	6	7	8
1	0.499	0.500	0.000	0.000	0.001	0.000	0.000	0.000
2	0.000	0.500	0.495	0.001	0.001	0.001	0.001	0.001
3	0.000	0.001	0.840	0.153	0.001	0.001	0.001	0.001
4	0.000	0.003	0.003	0.957	0.001	0.034	0.001	0.001
5	0.000	0.308	0.000	0.000	0.614	0.077	0.001	0.000
6	0.000	0.000	0.000	0.333	0.000	0.666	0.001	0.000
7	0.001	0.001	0.001	0.001	0.001	0.001	0.993	0.001
8	0.001	0.001	0.001	0.001	0.000	0.001	0.001	0.994

depths. Some have depths of 28.8 m, others are somewhat shorter: about 19.2 m in depth. Vertical transition probabilities are estimated over a sampling interval of 0.3 m. This sampling corresponds to the minimum thickness of a layer observed in the borehole. Table 6 displays the vertical transition probability matrix calculated from 19 boreholes.

The vertical transition probability matrix has a special structure. It is clustered, i.e., one may observe that states from 1 to 5 are interacting with each other: their entries are non-zero. There are some other transitions which are zeros, or almost zeros (e.g., transitions from states 1 to 5 and 6 to 13). This is due to the fact that some lithologies are present in the top of the image (e.g., 1–5), and are not present in the bottom of the image and vice versa. It is noticeable that states 1–5 are present at the top of the image and states 6–10 are present at the bottom of the image. This type of non-stationary data set is typical in many geological deposits.

The first simulation is performed on the basis of calculating the vertical transition probabilities from all boreholes with various depths. The postulated forward horizontal transition probability matrix is set to be a symmetric and diagonally dominant matrix as in the previous case study. The justification of this choice is based on the lack of information about the horizontal variability and the common knowledge about subsurface with a layering structure: this means highly diagonal elements in terms of transition probability matrix. The diagonal elements are chosen equal to $p^h{}_{ii} = 0.988$ and off-diagonal elements are given equal probabilities: $p^h_{ij} = (1 - p^h_{ii})/(n - 1) = 0.001$ where $n = 13$. The results of the simulation are shown in Figure 10a and b. They show similar geological configurations as the one drawn by the geologists (Figure 9 top image). It is important to notice that the simulation reproduces the white top and bottom spaces as shown in Section A–B. This means that the concept of having fictitious states to model the sky and the deep ground works, and the model is capable of handling any top or bottom topography.

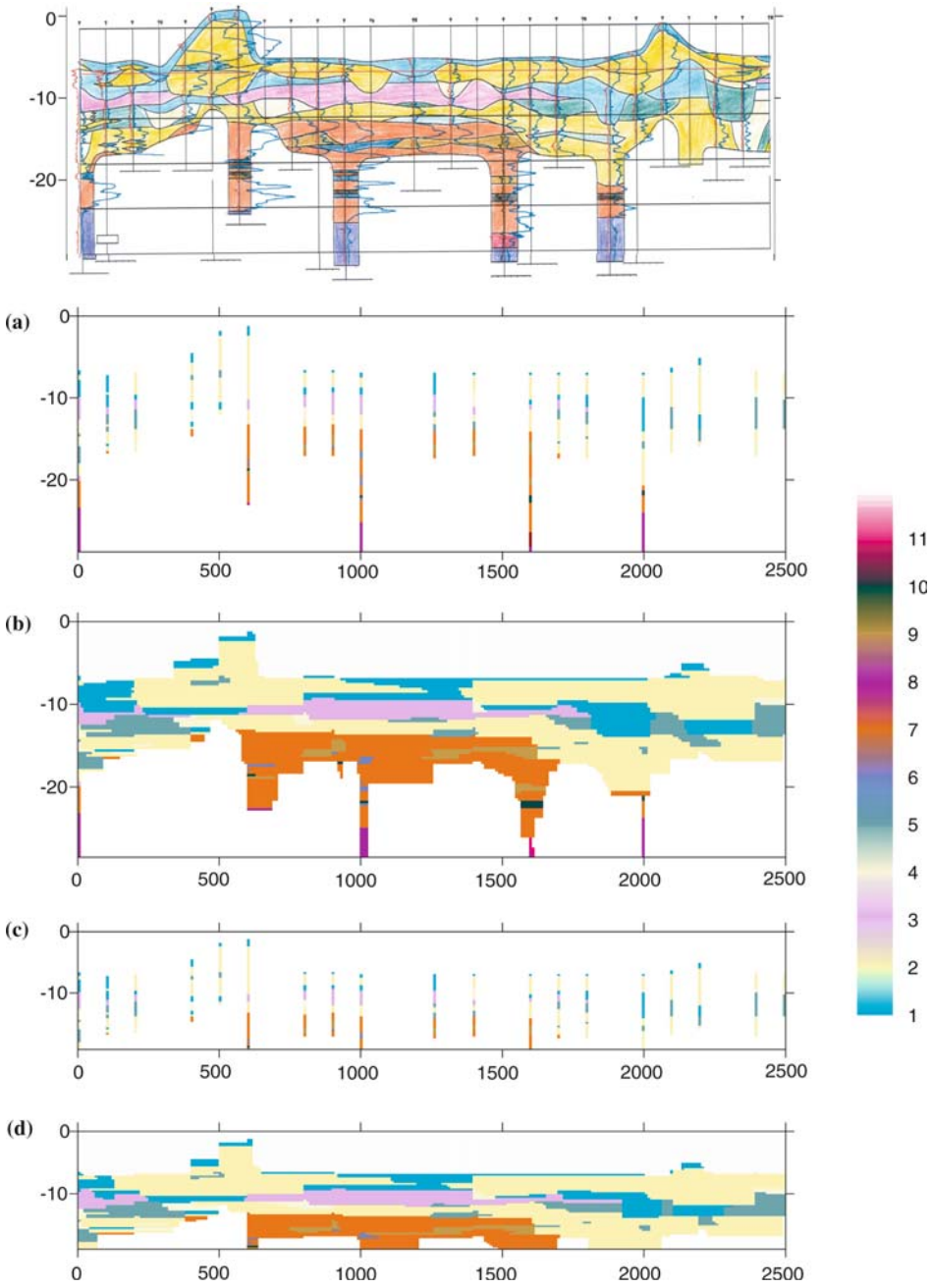

Figure 10. Stochastic simulation of the longitudinal section (A–B) of afsluitdijk-Caspar de Roblesdijk, a part of Waddenzeedijken conditioned on 19 boreholes. Top image shows the geological section drawn by geologists. Image (a) shows 19 boreholes data. Image (b) shows a simulation conditioned on 19 boreholes (using forward CMC model). Image (c) shows 19 boreholes of the upper part of the A–B section. Image (d) shows the corresponding simulation of the upper part conditioned on 19 boreholes.

Table 6. Vertical transition probability matrix estimated over sampling intervals of 0.3 m form 19 boreholes

	State												
State	1	2	3	4	5	6	7	8	9	10	11	12	13
1	0.696	0.186	0.098	0.010	0.010	0.000	0.000	0.000	0.000	0.000	0.000	0.000	0.000
2	0.045	0.849	0.006	0.016	0.033	0.000	0.029	0.000	0.000	0.000	0.000	0.003	0.019
3	0.000	0.081	0.790	0.032	0.081	0.000	0.016	0.000	0.000	0.000	0.000	0.000	0.000
4	0.030	0.121	0.031	0.727	0.091	0.000	0.000	0.000	0.000	0.000	0.000	0.000	0.000
5	0.000	0.171	0.000	0.011	0.784	0.000	0.023	0.000	0.000	0.000	0.000	0.000	0.011
6	0.000	0.000	0.000	0.000	0.000	0.300	0.700	0.000	0.000	0.000	0.000	0.000	0.000
7	0.000	0.000	0.000	0.000	0.000	0.036	0.813	0.022	0.043	0.029	0.007	0.000	0.050
8	0.000	0.000	0.000	0.000	0.000	0.000	0.000	0.889	0.000	0.000	0.000	0.000	0.111
9	0.000	0.000	0.000	0.000	0.000	0.043	0.261	0.000	0.696	0.000	0.000	0.000	0.000
10	0.000	0.000	0.000	0.000	0.000	0.143	0.285	0.000	0.143	0.429	0.000	0.000	0.000
11	0.000	0.000	0.000	0.000	0.000	0.000	0.000	0.000	0.001	0.001	0.998	0.000	0.000
12	0.042	0.008	0.000	0.000	0.000	0.000	0.000	0.000	0.000	0.000	0.000	0.950	0.000
13	0.000	0.000	0.000	0.000	0.000	0.000	0.000	0.000	0.000	0.000	0.001	0.001	0.998

10.7. SPLITTING THE CROSS-SECTION

Because of the different depths of CPT profiles, it is decided to split the section horizontally into two parts: an upper part of depth of 19.2 m and a lower part with a depth of 14.4 m. Figure 10 (c) shows the upper part. The vertical transition probability matrix for the upper part is calculated and given in Table 7. This matrix is not significantly different from the vertical transition probability matrix for the whole section (Table 6), except that states 8, 10 and 11 are not present any more.

Simulation results are displayed in Figure 10(d) for the upper part. The results are similar to the case where the transition probabilities are calculated from the whole depth of the boreholes. This is due to the fact that the vertical transitions on the upper part are almost identical to the ones calculated from the overall depth of the boreholes. The application of the model on this data set shows consistency in the model performance.

10.8. HORIZONTAL SAMPLING INTERVALS

We investigated the optimum sampling interval that is suitable in the horizontal direction. In this experiment, 13 boreholes are used for conditioning to speed up the simulations since there is no significant difference in the simulation results between 19 and 13 boreholes. The horizontal transition probability matrix is symmetrical and diagonally dominant with $p_{ii} = 0.988$. Sampling intervals of 5, 10, 20, 40, and 100 m are investigated. Figure 11 shows the simulation results. There is no significant difference between the simulations. This means that for symmetric and highly diagonally dominant horizontal transition probability

Table 7. Vertical transition probability matrix estimated over a sampling interval of 0.3 m for the upper part of the image from 19 boreholes from Figure 10c

	State									
State	1	2	3	4	5	6	7	9	12	13
1	0.696	0.186	0.098	0.010	0.010	0.000	0.000	0.000	0.000	0.000
2	0.046	0.854	0.003	0.017	0.033	0.000	0.026	0.000	0.000	0.020
3	0.000	0.083	0.800	0.033	0.083	0.000	0.000	0.000	0.000	0.000
4	0.030	0.121	0.030	0.727	0.091	0.000	0.000	0.000	0.000	0.000
5	0.000	0.170	0.000	0.011	0.784	0.000	0.023	0.000	0.000	0.011
6	0.000	0.000	0.000	0.000	0.000	0.333	0.667	0.000	0.000	0.000
7	0.000	0.000	0.000	0.000	0.000	0.038	0.797	0.076	0.000	0.089
9	0.000	0.000	0.000	0.000	0.000	0.053	0.211	00.00	0.000	0.000
12	0.042	0.008	0.000	0.000	0.000	0.000	0.000	0.000	0.950	0.000
13	0.000	0.000	0.000	0.000	0.000	0.000	0.001	0.001	0.000	0.998

Domain dimensions 2500×19.2 m.

matrices, changing the horizontal sampling intervals does not influence the results. However, the entropy maps show reduction of uncertainty with increasing sampling intervals. This demonstrates the usefulness of the entropy maps to quantify uncertainties.

10.9. WALTHER'S LAW

In this experiment, we investigated the use of the downward vertical transition probability matrix in the horizontal direction with different sampling intervals. Conditioning is performed on 13 boreholes as in the previous experiment. Figure 12 shows simulation results based on that concept. Four sampling intervals are utilized ranging from 10, 20, 40, and 100 m. Best results in terms of connectivity and similarity to geologist predictions is observed with $dx = 100$. Entropy maps (Figure 12 left column) emphasised the reduction of uncertainty by increasing the sampling intervals.

10.10. COMPARISON OF VARIOUS COUPLED MARKOV CHAIN MODELS (FCMC, BCMC AND FBCMC)

Figure 13 shows the application of FCMC, BCMC, and FBCMC with conditioning on 8 and 13 boreholes, respectively. The sampling interval is set to 10 m, and a highly diagonally dominant horizontal transition probability matrix with $p_{ii}^{h} = 0.988$ is applied. The results show that conditioning on less boreholes leads to more connectivity of the geological units. This is accounted for by the high diagonal dominancy of the transition probability matrix. There is no noticeable difference between FCMC, BCMC, and FBCMC in terms of geological configurations. This is mainly due to the horizontal layering structure of the site.

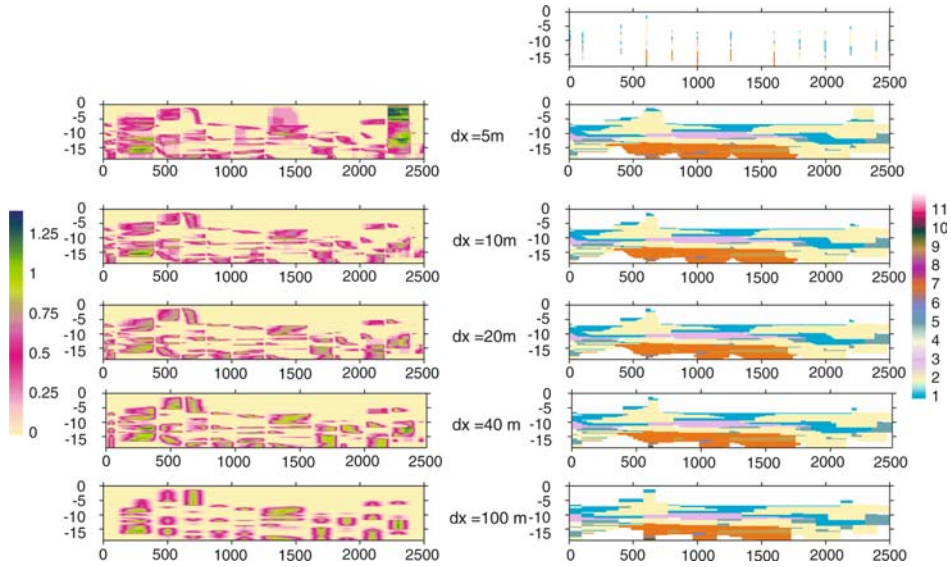

Figure 11. Sensitivity analysis of the horizontal sampling intervals using a fixed symmetric horizontal transition probability matrix with diagonal elements $p_{ii}^{h} = 0.988$. The top right most image shows 13 boreholes. The rest of the images are final images generated by the FCMC model based on 30 realizations and conditioned on 13 boreholes with different horizontal sampling intervals (right column), and empirical entropy (left column).

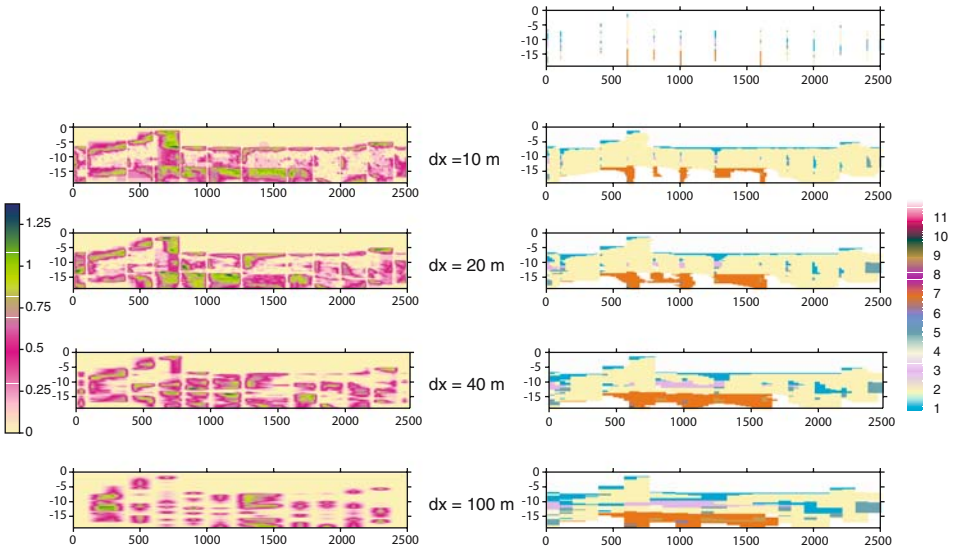

Figure 12. Sensitivity analysis on the application of Walther's Law. The images are generated with a subtle modification of vertical transition probabilities (reducing some zeros) for application in the horizontal direction with different sampling intervals ranging from 10, 20, 40 and 100 m respectively. The right column shows the final simulation images and the left column shows the empirical entropy maps.

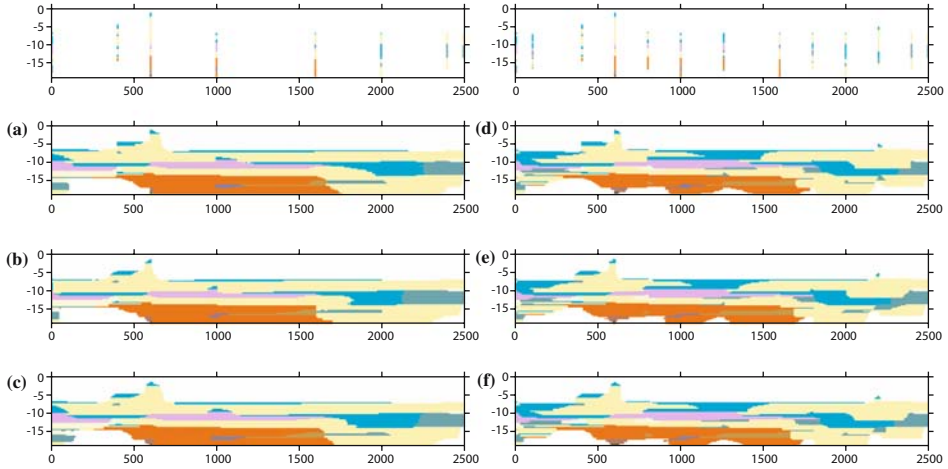

Figure 13. Comparison between various coupled Markov chains models conditioned on eight boreholes (left column): (a) FCMC, (b) BCMC and (c) FBCMC and 13 boreholes (right column): (d) FCMC, (e) BCMC and (f) FBCMC respectively.

10.11. EFFECT OF CONDITIONING ON THE NUMBER OF BOREHOLES

Figure 14 shows simulation results performed using FCMC with a high diagonal dominancy horizontal transition probability matrix ($p^h_{ii} = 0.988$), a horizontal sampling interval of 10 m, and conditioning on a number of boreholes of 8, 13, and 19, respectively. It is obvious that increasing the number of boreholes leads to improving the simulation results. There is no noticeable difference when conditioning is performed on 13 or 19 boreholes. This means that 13 boreholes were sufficient to characterize the heterogeneity at the site.

10.12. SITE DESCRIPTION AND PARAMETER ESTIMATION

Another application is made at the Delaware River and its underlying aquifer system in the vicinity of the Camden metropolitan area, New Jersey, USA. Data used is collected from the literature (Navoy, 1991). The geological units associated with the aquifer system in the vicinity of the Camden metropolitan area are shown in Figures 15 and 16. We give a short description of the lithologies that control the hydrological properties. The bed rock consists of crystalline rocks of Precambrian to Paleozoic age. A thick sequence of non-marine gravels, sands, silts and clays is deposited upon the bedrock surface. These sediments are fluvial-deltaic and represent deposition within a sub-aerial delta plain (Owen and Sohl, 1969). The gravel and sand units are channel fill deposits, and some of the finer-grained deposits are not extensive and often occur in minor lenses. There are however, two laterally extensive clay units within the formation. These clay units extend over a wide area and may

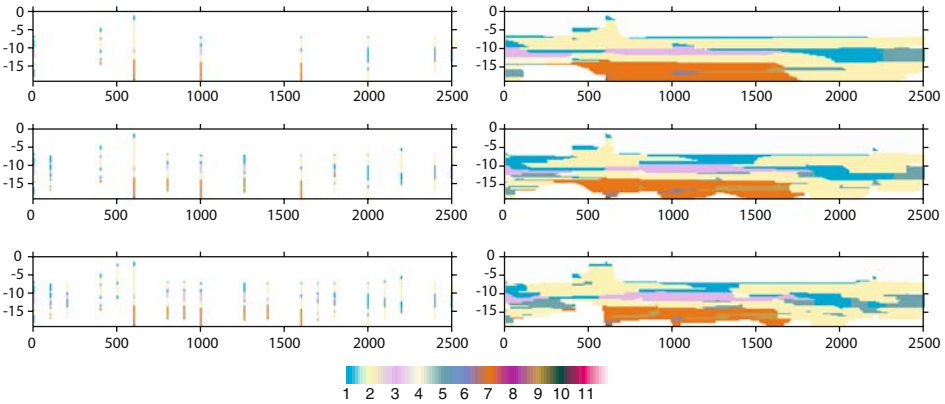

Figure 14. Effect of number of conditioning boreholes (eight boreholes 'first row', 13 boreholes 'second row' and 19 boreholes 'third row' respectively) using FCMC on the performance of the model.

represent extra basinal changes (Navoy, 1991). Hydrogeological studies show that the aquifer system at the site consists of upper, middle and lower sand aquifers separated by two confining units as shown in Figure 15.

For simulation of aquifer heterogeneity, a distinction of the various lithologies is made (Navoy, 1991). Seven lithologies are considered. These lithologies are coded according to Table 8. Two sections are considered. A cross-section A–A′ perpendicular to the river and a longitudinal section F–F′ along the river, shown in Figure 15 and Figure 16, respectively. The sections cover an area of 20320×368 ft. ($6193.2 \text{ m} \times 112.1 \text{ m}$) for section A–A′ and an area of 151166.7×350 ft.

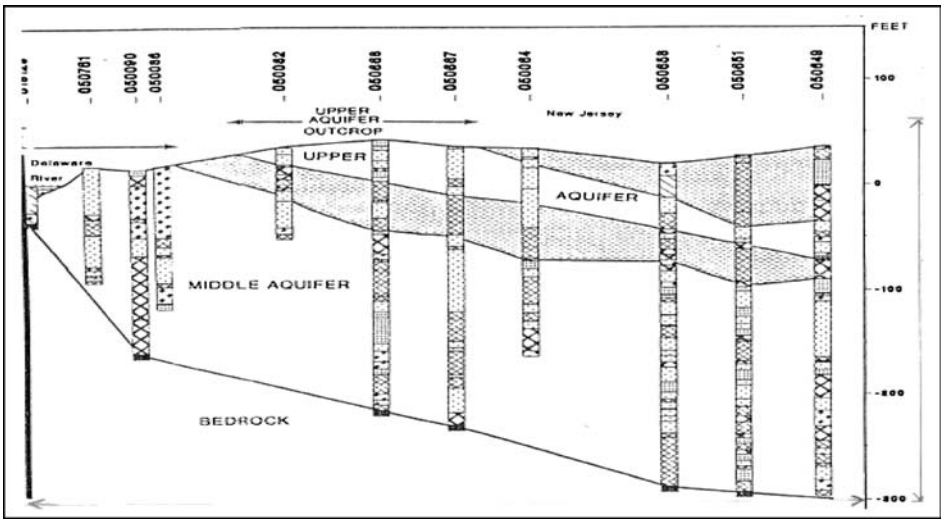

Figure 15. Cross-section A-A′ of the Delaware River and its underlying aquifer system in the vicinity of the Camden metroplitan area, New Jersey (from Navoy, 1991).

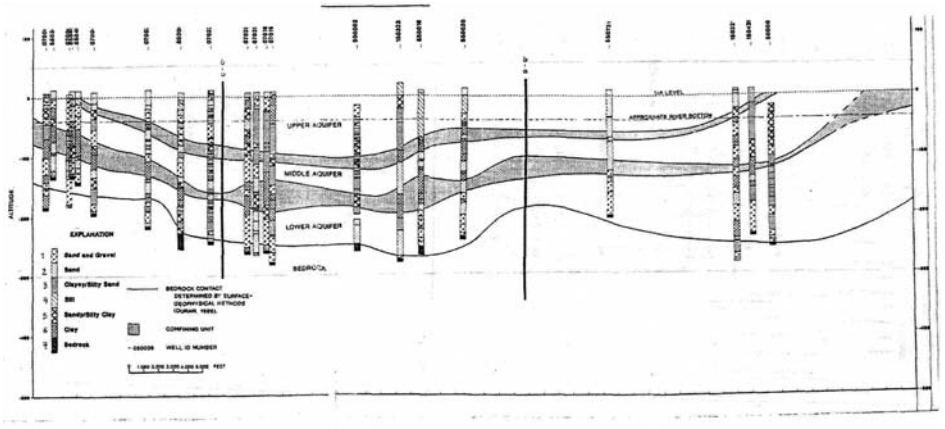

Figure 16. Longitudinal section F-F′ of the Delaware River and its underlying aquifer system in the vicinity of the Camden metroplitan area, New Jersey (from Navoy, 1991).

(46073.4 m × 106.7 m) for section F–F′. Boreholes are shown in the figures. Section A–A′ contains 11 boreholes and section F–F′ contains 21 boreholes. The sampling interval in the vertical direction is chosen equal to 4 ft, which corresponds to the smallest thickness observed in the boreholes. A sensitivity study similar to the previous cases is performed on sections A–A and F–F′, respectively. In this case study there are no geological maps to judge the model performance. Therefore, a cross-validation technique (referenced by Deutsch and Journel (1992)) is applied to evaluate the model performance.

10.13. SENSITIVITY ANALYSIS ON CROSS-SECTION A-A′ FOR THE DEGREE OF DIAGONAL DOMINANCY OF THE HORIZONTAL TRANSITION PROBABILITY MATRIX

A conditional simulation of section A–A′ is performed. The transition probability matrix in the vertical direction is calculated from the given 11 boreholes. table 10 presents the vertical transition probability matrix calculated over sampling intervals of 4 ft.

Figure 17 shows simulation results, which have been performed using a diagonally dominant horizontal transition probability matrix over a horizontal sampling

Table 8. Coding of lithologies in aquifer system

Lithology	Code
Sand and gravel	1
Sand	2
Clayey/silty sand	3
Silt	4
Sandy/silty clay	5
Clay	6
Bedrock	7

interval of 80 ft, coupled with the vertical one in Table 9. The diagonal elements are chosen as $p_{ii}^h = 0.603$, 0.699, 0.801, 0.908 and 0.986, respectively. The off-diagonal elements of the real states (from 1 to 7) are calculated from $p_{ii}^h = 1 - (p_{ii}^h/(n-2) + 0.001)$, where the value 0.001 is the transition probability p_{i8}^h from any state to the artificial state 8 for $i = 1,\ldots,7$ and therefore, $p_{88}^h = 0.993$. It is obvious that increasing the diagonal elements leads to higher connectivity of the geological units (Figure 17 right column), and reduction in the local entropy (Figure 17 left column).

10.14. WALTHER'S LAW AND HORIZONTAL SAMPLING INTERVALS

Figure 18 shows simulation results performed using four different sampling intervals of 40, 80, 280, and 400 ft, respectively, and a horizontal transition probability matrix that is equal to the vertical one (Table 9).The results have noisy and inclined features at small sampling intervals. The noise smears out for large sampling intervals at 280 ft and the inclination levels off. The inclination in the results has two reasons: First, the geometrical condition due to the unilateral character of the coupled Markov chain model. Second, a probabilistic condition which plays a role when high

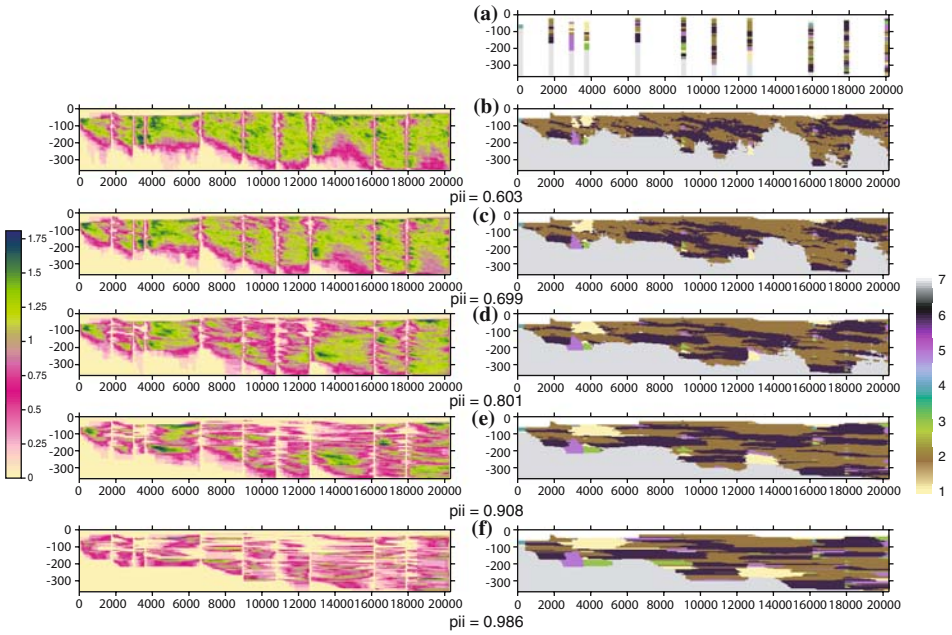

Figure 17. Sensitivity analysis (for section A-A′) for the degree of diagonal dominancy of the horizontal transition probability matrix. Top right image shows the 11 boreholes. The images b, c, d and e with $p_{ii}^h = 0.603$, 0.699, 0.801, 0.9, 0.908 and 0.986, respectively are the images generated by the FCMC model based on 30 realizations, and conditioned on 11 boreholes using horizontal and diagonally dominant transition probability matrices over a horizontal sampling interval of 80 f. Left columns show the corresponding empirical entropy maps.

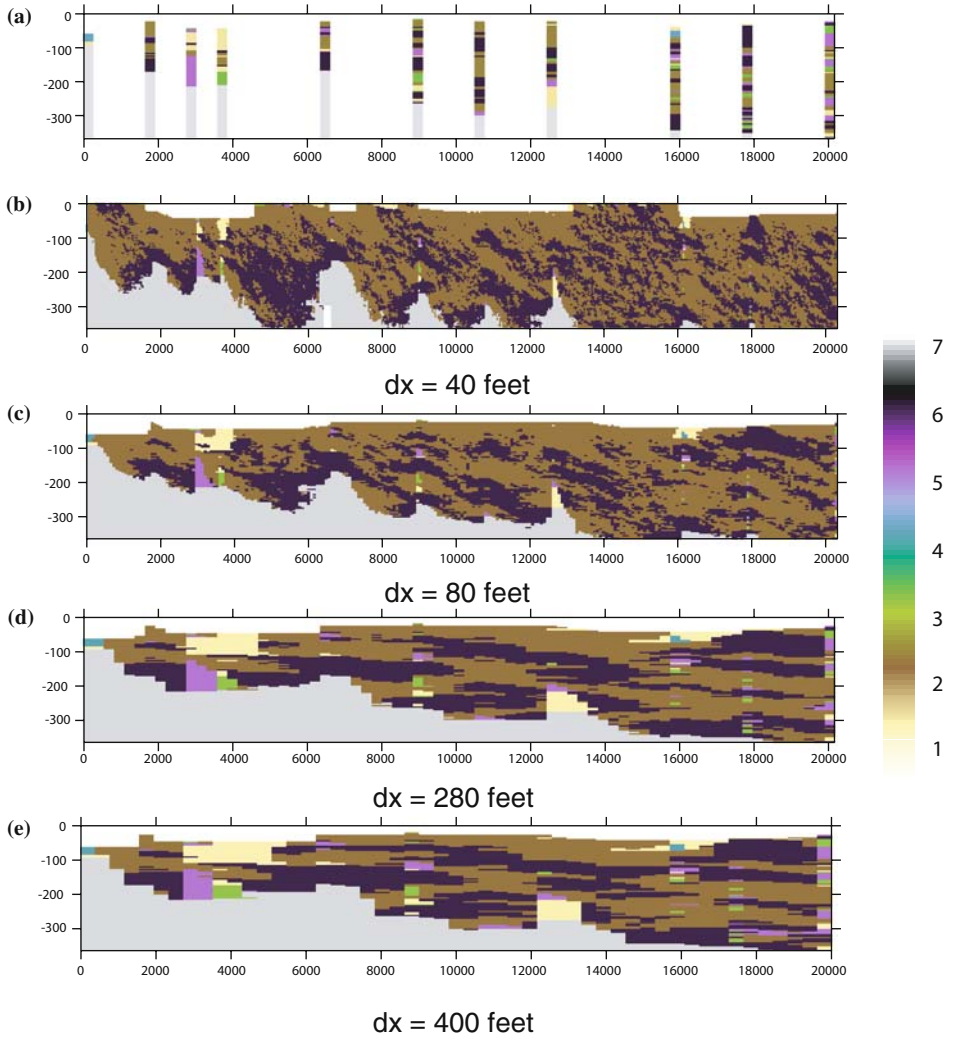

Figure 18. Sensitivity analysis (for section A-A′) for horizontal sampling intervals using a fixed horizontal transition probability matrix which is equal to the vertical one (Application of Walther's law). Top image shows the 11 boreholes, and the rest are images generated by the FCMC model based on 30 realizations and conditioned on 11 boreholes with different horizontal sampling intervals.

diagonal elements of transition probability matrices in both vertical and horizontal directions are used. The noise at small sampling intervals is due to the high number of multiplications of the transition matrix by itself. This can lead to the stationary distribution of the chain, and generation of cells that are no longer dependent on borehole information. It is worth mentioning that the simulation in Figure 17(e) with $p_{ii}^{h} = 0.908$ and a horizontal sampling interval of $dx = 80$ ft is similar to simulation results in Figure 17(d) with $p_{ik}^{h} = p_{ik}^{v}$ and $dx = 280$ ft. This leads to the conclusion that similar simulation results, in terms of geological configurations, can

Table 9. Vertical transition probability matrix sampled over 4 ft (for section A–A′)

	State							
State	1	2	3	4	5	6	7	8
1	0.724	0.066	0.053	0.013	0.026	0.092	0.026	0.000
2	0.044	0.759	0.030	0.000	0.034	0.133	0.000	0.000
3	0.000	0.180	0.620	0.000	0.100	0.080	0.020	0.000
4	0.091	0.091	0.000	0.818	0.000	0.000	0.000	0.000
5	0.048	0.096	0.036	0.000	0.711	0.084	0.024	0.000
6	0.022	0.124	0.022	0.000	0.051	0.753	0.028	0.000
7	0.000	0.000	0.000	0.000	0.000	0.000	1.000	0.000
8	0.026	0.051	0.026	0.013	0.013	0.000	0.000	0.872

be reached by using a diagonally dominant horizontal transition probability matrix with small sampling intervals, or by using almost identical horizontal and vertical transition probability matrices with larger sampling intervals.

10.15. COMPARISON OF VARIOUS COUPLED MARKOV CHAIN MODELS (FCMC, BCMC AND FBCMC)

Figure 19 shows a comparison between various coupled Markov chain models on section A–A′. The three methods FCMC, BCMC and FBCMC are applied conditioned on 11 boreholes with forward horizontal transition probability matrix equal to the vertical one over a sampling interval of 280 ft. Generally speaking, there is no noticeable difference between the three models. However, one could notice some differences between the three models when the conditioning boreholes are far apart. Figure 19 with FCMC shows inclination from left to right of the black lithology. There is a slit inclination from right to left in Figure 19 with the backward model (BCMC), and there is a wavy pattern in Figure 19 with the forward–backward model (FBCMC). This behaviour is due to the geometrical character of these models (asymmetry) which is adapted to fit borehole data and values of the transition probabilities. This leads us to rely on some prior information about the sedimentation direction before one implements one of these models.

10.16. CROSS-VALIDATION

Figure 20 shows the application of the so-called "cross-validation" technique (referenced by Deutsch and Journel (1992)) on section A–A′. In this technique, one systematically excludes some of the data from the given data set (boreholes), and performs the simulation using the remaining data, and then simulates the data that was excluded. In this way, a judgment of the model performance can be made. In section A–A′, seven boreholes are considered for performing conditioning. These

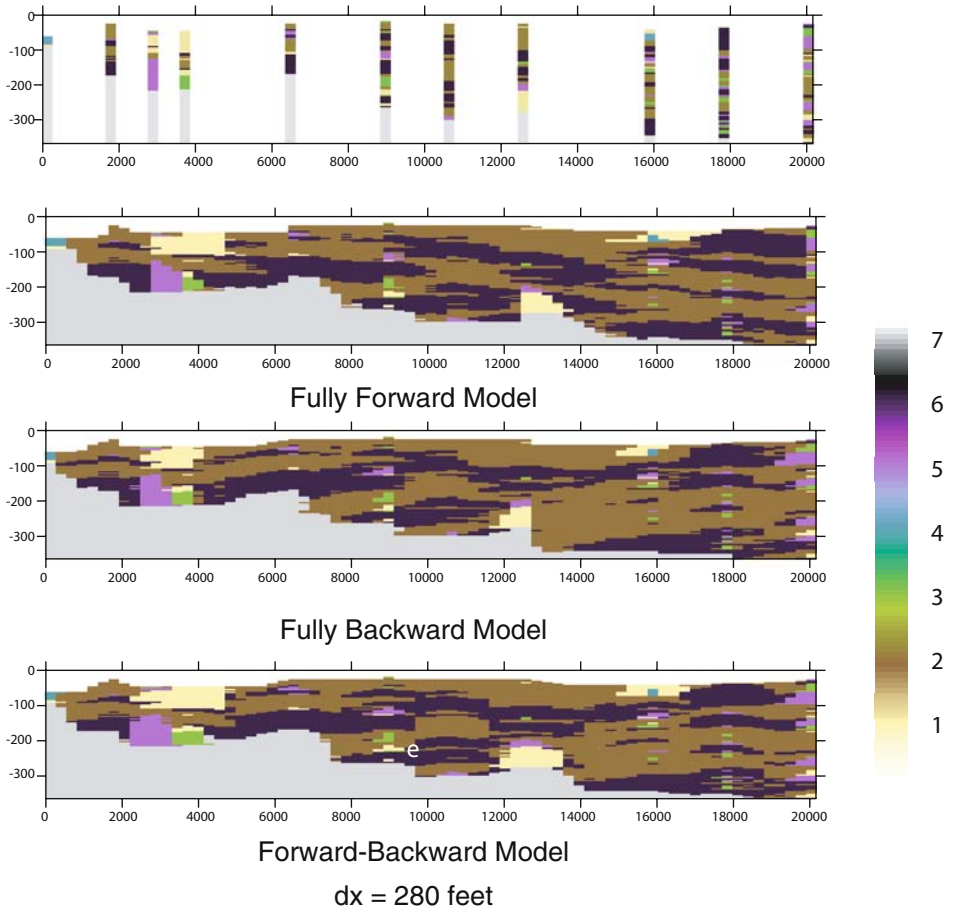

Figure 19. Comparison of various models for section A-A′. Top right most image shows 11 boreholes. The first row shows the simulation with FCMC model. Horizontal sampling intervals=280 feet and fixed horizontal transition probability matrix equals vertical probability matrix. Second row shows the simulation with BCMC and last row shows FBCMC simulation.

boreholes are shown in Figure 20, while the rest of boreholes are simulated (four boreholes) using the three models. The simulated boreholes are rather satisfactory. There are mismatches between boreholes data and the simulated boreholes. The influence of directionality is more stronger in this case when compared with the case of conditioning on the 11 boreholes. This emphasizes that increasing the distance between boreholes leads to a stronger directional dependency.

10.17. SENSITIVITY ANALYSIS OF SECTION F–F′

For simulation of section F–F′, the vertical transition probability matrix is calculated from 21 boreholes and given in Table 10. Figure 21 shows simulation results

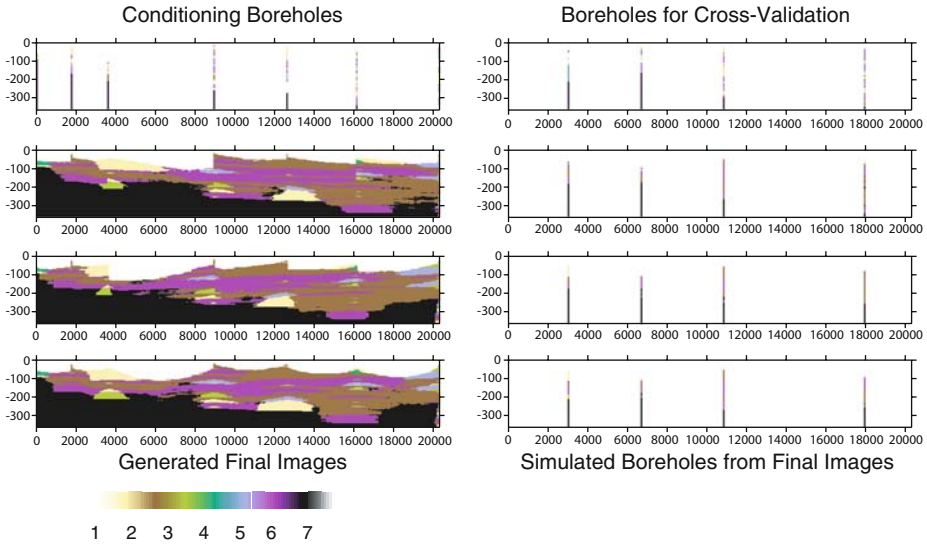

Figure 20. Cross-validation for section A-A'. Top left image shows seven conditioning boreholes. Top right most shows boreholes for cross-validation. The second row left column shows the simulation with FCMC model conditioned on seven boreholes (right image shows the simulated boreholes). The third row left image shows the simulation with BCMC model conditioned on seven boreholes (right image shows the simulated boreholes). The last row left column shows the simulation with FBCMC model conditioned on seven boreholes (right image shows the simulated boreholes).

performed using four different sampling intervals of 100, 200, 400, and 800 ft, respectively, and a horizontal transition probability matrix that is equal to the vertical one (Table 10), with subtle changes of some 0's to 0.001. The results with small sampling intervals show strong inclinations. As might be expected, the inclination decreases with increased sampling. Figure 22 shows simulation results which have been performed on section F–F′ using diagonally dominant transition probability matrices in the horizontal direction, and horizontal sampling interval of 80 ft. Increasing the degree of diagonal dominancy reduces the inclination angle of the geological structures and the entropy decreases. Figure 23 shows simulation results of FCMC, BCMC and FBCMC conditioned on 21 boreholes. Simulations show different orientation in the predicted geological configurations. This behaviour is due to the geometrical character of the CMC model (asymmetry) which is adapted to fit borehole data and the values of the diagonal elements of the transition probabilities.

Figure 24 shows the relation between the tangent of the angle of inclination and the horizontal scale of the site from some collected data in this study, and a study made on the MADE site (Elfeki and Rajabiani, 2002). The graph shows that at large scales the angle is almost zero, showing a layered structure. However, at small scales the angle increases. From an engineering point of view, it could be useful to find an empirical relation between the scale of the site and the relation between the horizontal and vertical sampling intervals. This would help to use the vertical transition

Table 10 Vertical transition probability matrix sampled over 4 ft (for section F–F′)

	State							
State	1	2	3	4	5	6	7	8
1	0.800	0.047	0.030	0.003	0.020	0.083	0.017	0.000
2	0.074	0.754	0.039	0.027	0.043	0.051	0.012	0.000
3	0.073	0.056	0.789	0.000	0.047	0.026	0.009	0.000
4	0.045	0.068	0.045	0.795	0.023	0.023	0.000	0.000
5	0.048	0.096	0.036	0.000	0.711	0.084	0.024	0.000
6	0.054	0.061	0.034	0.000	0.027	0.797	0.027	0.000
7	0.000	0.000	0.000	0.000	0.000	0.000	1.000	0.000
8	0.008	0.055	0.013	0.004	0.008	0.000	0.000	0.911

probability matrix in the horizontal direction with some scaling of the vertical transition and would make use of Walther's law in a quantitative sense. However, it will still need further application of the CMC model at various sites to establish this relation.

11. Conclusions

This research focused on an extension and intensive applications of the two-dimensional coupled Markov chain model developed by Elfeki and Dekking (2001). Three computer codes have been developed to implement different coupled Markov chain algorithms. Namely, the fully forward-coupled Markov model that is referred to as (FCMC), the fully backward-coupled Markov model (BCMC), and the forward-backward model (FBCMC). Many issues are addressed, such as: sensitivity analysis of optimal sampling intervals in horizontal and lateral directions, directional dependency, various horizontal transition probability matrices, degree of diagonal dominancy of the horizontal transition matrix, use of Walther's law to describe lateral variability, effect of conditioning on number of boreholes, stability of the Monte Carlo realizations various implementation strategies, use of cross validation techniques to evaluate model performance and image division for statistically non-homogeneous deposits. The choice between these models for field applications depends on geological knowledge such as the direction of the sedimentation process in the fluvial environment. The following conclusions can be made for these case studies:

1. Entropy maps are good tools to show places where high and low uncertainties are present, so can be used for the design of sampling networks to reduce uncertainty at highly uncertain locations. It can also be useful in order to make an optimal choice of the locations of a new borehole.
2. Symmetrical and diagonally dominant horizontal transition probability matrices over a proper horizontal sampling interval provide plausible results from a geological point of view. In the Afsluitdijk-Lemmer and Afsluitdijk-Caspar de Roblesdijk case studies, symmetrical and diagonally dominant horizontal tran-

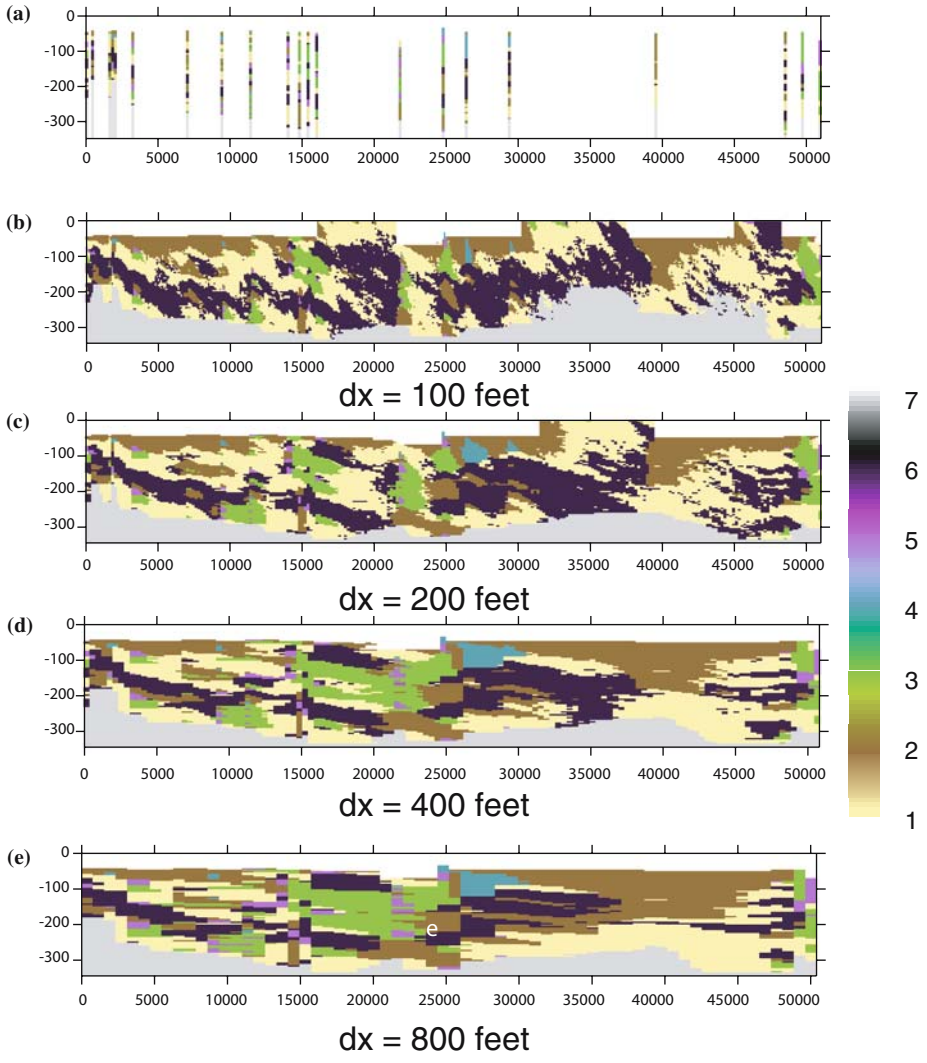

Figure 21. Sensitivity analysis (for section F-F') on horizontal sampling intervals using a fixed horizontal transition probability matrix, which is equal to the vertical one (Application of Walther's law). Top image shows the 21 boreholes, and the rest are the images generated by the FCMC model based on 30 realizations and conditioned on 21 boreholes with different horizontal sampling intervals.

sition probability matrices ($p_{ii}^h = 0.993$ and 0.988, respectively) over a sampling interval of 10 m seem to give fairly good results when compared with geologist predictions.

3. The choice of sampling intervals in the horizontal direction is crucial. But this choice can only be made by performing a sensitivity analysis using several sampling intervals. Very small sampling intervals with respect to the distance

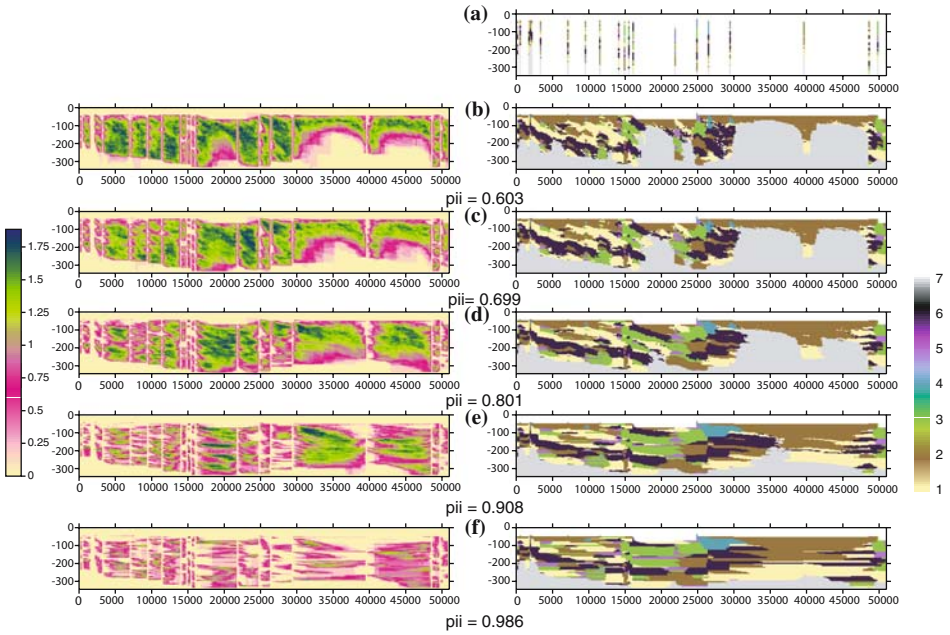

Figure 22. Sensitivity analysis (for section F-F') on the degree of diagonal dominancy of the horizontal transition probability matrix. Top right image shows 21 boreholes. The images b, c, d E and f with p_{ii}^{h}= 0.603, 0.699, 0.801, 0.908 and 0.986, respectively are the images generated by the FCMC model based on 30 realizations and conditioned on 21 boreholes using horizontal and diagonally dominant transition probability matrices. The left column shows the corresponding empirical entropy maps.

between the boreholes will lead to loss of lateral continuity of the geological features. However, very long sampling intervals will lead to unrealistic connectedness. For Afsluitdijk-Lemmer and Afsluitdijk-Caspar de Roblesdijk a value of 10 m is a reasonable choice.

4. Heavily sampled sites may have redundant data that does not improve site characterization. For Afsluitdijk-Caspar de Roblesdijk, 13 boreholes over a distance of 2500 m (out of 19) are sufficient to delineate the global geological configuration at the site. The concept of data redundancy is also supported by early work by Eggleston et al. (1996) at Cape Cod and Borden site.
5. Application of Markov models on the Delaware river and its underlying aquifer system (section A–A′) shows that with a horizontal transition probability matrix that is equal to the vertical one, small sampling intervals (40 f) lead to noisy and highly inclined geological features while, large sampling intervals (280 and 400 f) produce lateral continuity of the geological features and less inclination.
6. Similar simulation results, in terms of geological configurations, can be obtained by using a diagonally dominant horizontal transition probability matrix with small sampling intervals, or by using almost identical horizontal and vertical transition probability matrices with larger sampling intervals. For section A–A′ in the Delaware river case study, similar simulation results are

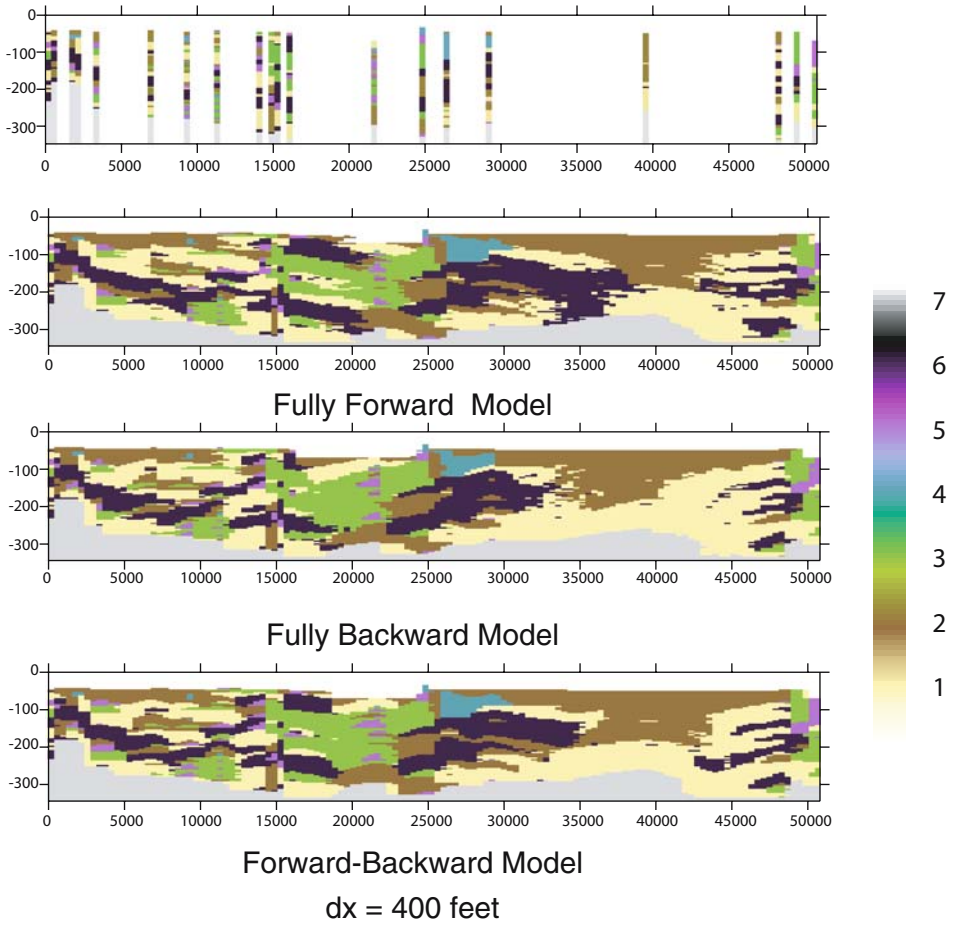

Figure 23. Comparison of various models for section F-F'. Top right most image shows 21 boreholes. The first row is the simulation with FCMC model. Horizontal sampling intervals=400 f and fixed horizontal transition probability matrix equals the vertical probability matrix. Second row shows the simulation with BCMC and last row shows FBCMC simulation.

reached when using a diagonally dominant horizontal transition probability matrix with sampling intervals of 80 ft, and horizontal transition probability matrix equal to the vertical transition probability matrix with sampling intervals of 280 or 400 ft.

7. FCMC, BCMC and FBCMC with the same horizontal and vertical transition probability matrices with horizontal sampling intervals of 280 f do not show any noticeable difference in terms of global geological features for section A–A′.
8. The so-called ''cross-validation'' technique (referenced by Deutsch and Journel (1992)) seems satisfactory for validation of Markov models. However, a quantitative measure should be assigned to evaluate the model performance. This will be considered in future research.

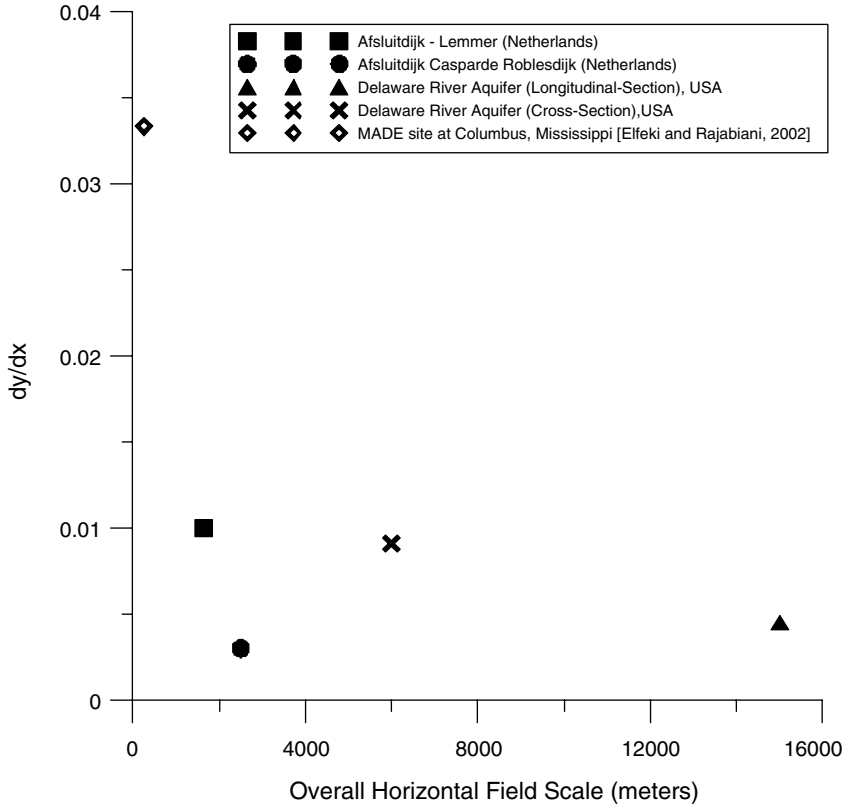

Figure 24. Relation between the angle of inclination of the geological structure and the field scale of the site.

9. Application of various coupled Markov chain models on section F–F′ shows noticeable differences in the simulation results in the regions with less boreholes. However, there is no significant difference in regions with dense boreholes. This behaviour is due to the geometrical character of these models (asymmetry), which is adapted to fit borehole data, values of transition probabilities and sizes of the sampling intervals. This leads to the conclusion that prior knowledge about the sedimentation direction can be helpful when there is lack of boreholes to decide about which model can be used.
10. The concept of having fictitious states to model the sky and the deep ground works and the model is capable of handling any top or bottom topography.

Appendix: The Backward Chain

It is known that in case the chain is aperiodic and irreducible, the stationary probabilities w_l of the chain exist, and are all strictly positive. In this case the backward chain has transition probabilities,

$$\overleftarrow{p}_{kl} = \frac{w_l}{w_k} p_{lk},$$

and since the same formula holds for the N-step transition probabilities we can derive Equation (6) directly from Equation (3):

$$\overleftarrow{p}_{qr|a} = \frac{\overleftarrow{p}_{qr}\overleftarrow{p}_{ra}^{(N-1)}}{\overleftarrow{p}_{qa}} = \frac{\frac{w_r}{w_q} p_{rq} \cdot \frac{w_a}{w_r} p_{ar}^{(N-1)}}{\frac{w_a}{w_q} p_{aq}^{(N)}} = \frac{p_{rq} p_{ar}^{(N-1)}}{p_{aq}^{(N)}}.$$

Acknowledgements

The authors would like to thank GeoDelft for providing the data of the Dutch sites, and are grateful to Ir. Hamid Rajabiani for some preliminary simulations using the computer codes developed by the first author. The authors would like also to thank the anonymous referees for their valuable comments.

References

Arndt, C. (2001) *Information measures. Information and its description in science and engineering*, Springer-Verlag, Berlin, ISBN 3-540-41633-1.

Bierkens, M. F. P. (1994) Complex confining layers: a stochastic analysis of hydraulic properties at various scales, PhD thesis, Utrecht university, Utrecht, The Netherlands, 263p.

Billingsley, P. (1995) *Probability and measure*, 3rd edition, Wiley-Interscience publication, John Wiley and Sons, New york.

Carle, S. F., and Fogg, G. E. (1996) Transition probability-based indicator geostatistics, *Mathematical Geology*, **28**(4), 453–476.

Carle, S. F., LaBolle, E. M., Weissmann, G. S. VanBrocklin D. and Fogg, G. E. (1998) Conditional simulation of hydrofacies architecture: A transition probability/Markov approach, In G. S. Fraser and J. M. Davis (eds.), Hydrogeologic Models of Sedimentary Aquifers, SEPM Concepts in Hydrol. Environ. Geol., *Soc. For Sediment. Geol.,* Tulsa, OK, Vol. 1, pp. 147–170.

Chessa A. (1995) Conditional simulation of spatial stochastic models for reservoir heterogeneity, PhD thesis, Delft University of Technology, The Netherlands.

Davis, J. C. (1986) *Statistics and Data Analysis in Geology*, New York, John Wiley and Sons, 646p.

Deutsch, C. V. and Journel, A. G. (1992) *GSLIB; Geostatistics Software Library and user's guide*, Oxford Univ. Press, New York, 340p.

Doveton, J. H. (1994) Theory and application of vertical variability measures from Markov chain analysis, In J.M. Yarus, and R.L. Chambers (eds.), Stochastic Modelling And Geostatistics- Principles, Methods and Case Studies: American Association Of Petroleum Geologists, Computer Methods In Geology, Vol. 3, pp 55–64.

Eggleston, J. R., Rojstaczer, S. A. and Peirce, J. J. (1996) Identification of hydraulic conductivity structure in sand and gravel aquifers: Cape cod data set, *Water Resources Research.*, **32**, (5), 1209–1222.

Elfeki, A. M. M. and Dekking, F. M. (2001) A Markov chain model for subsurface characterization: theory and applications, *Mathematical Geology*, **33**(5), 569–589.

Elfeki, A. M. M. and Rajabiani, H. R. (2002) Simulation of plume behavior at the macrodispersion experiment (Made1) site by applying the coupled Markov chain model for site characterization. In: *14th International Conference on Computational Methods in Water Resources "CMWR2002"*, Delft, The Netherlands Elsevier Publisher, pp. 655–662.

Haldorsen, H. H. and Damsleth, E. (1990) Stochastic modelling, *Journal of Petroleum Technology*, **42**(4), 404–412.

Krumbein, W. C. (1967) *Fortran Computer Program for Markov Chain Experiments in Geology: Computer Contribution 13*, Kansas geological survey, Lawrence, Kansas.

Middleton, G. V. (1973) Johannes Walther's law of the correlation of facies, *Geological Society of America, Bulletin,* **84**, 979–988.

Navoy, A. S. (1991) Aquifer-estuary Interaction and Vulnerability of Groundwater Supplies to sea level rise-driven saltwater intrusion, PhD Thesis, Pennsylvania State University, 225pp.

Owens, J. P. and Sohl, N. F. (1969) Shelf and deltaic paleo-environments in the Cretaceous-Tertiary formation of the New Jersey coastal plain In: Subitzky and Seymour (ed.), *Geology of the Selected Areas In New Jersey and Eastern Pennsylvania and Guidebook of Excursions: Geological Society of America And Associated Societies, November 1969, Annual Meeting,* Atlantic city, N.J., New Brunswick, N. J., Rutgers University Press, pp. 235–278.

Parks, K. P., Bentley, L. R. and Crowe, A. S. (2000) Capturing geological realism in stochastic simulations of rock systems with Markov statistics and simulated annealing, *Journal of Sedimentary Research,* **70**(4), 803–813.

Rajabiani, H. (2001) Characterization of subsurface heterogeneity from boreholes with coupled Markov chain for groundwater transport, MSc Thesis, Section Hydrology and Ecology, TU Delft, Delft, The Netherlands, 76p.

Wheatcraft, S. W. and Cushman, J. H. (1991) Hierarchical approaches to transport in heterogeneous porous media, *Reviews of Geophysics*, supplement, 263–269.